Kernel Three Pass Regression Filter

Rajveer Jat and Daanish Padha

University of California, Riverside

July 12, 2024

Abstract

We forecast a single time series using a high-dimensional set of predictors. When these predictors share common underlying dynamics, an approximate latent factor model provides a powerful characterization of their co-movements Bai (2003). These latent factors succinctly summarize the data and can also be used for prediction, alleviating the curse of dimensionality in high-dimensional prediction exercises, see Stock & Watson (2002a). However, forecasting using these latent factors suffers from two potential drawbacks. First, not all pervasive factors among the set of predictors may be relevant, and using all of them can lead to inefficient forecasts. The second shortcoming is the assumption of linear dependence of predictors on the underlying factors. The first issue can be addressed by using some form of supervision, which leads to the omission of irrelevant information. One example is the three-pass regression filter proposed by Kelly & Pruitt (2015). We extend their framework to cases where the form of dependence might be nonlinear by developing a new estimator, which we refer to as the Kernel Three-Pass Regression Filter (K3PRF). This alleviates the aforementioned second shortcoming. The estimator is computationally efficient and performs well empirically. The short-term performance matches or exceeds that of established models, while the long-term performance shows significant improvement.

Keywords: Forecasting, High dimension, Approximate factor model, Reproducing Kernel Hilbert space, Three-pass regression filter.

1 Introduction

In recent years, high-dimensional datasets have become increasingly accessible across various fields, including economics. It is widely acknowledged that estimation in high-dimensional settings poses a significant challenge known as the 'curse of dimensionality', which renders traditional finite-dimensional approaches ineffective.

Most modeling techniques applied to high-dimensional data assume the existence of a low-dimensional structure that effectively summarizes the data. One stylized feature of high-dimensional economic datasets is the presence of high and pervasive collinearity among variables, leading researchers to posit a data-generating process that assumes all variables are a function of a few latent factors. This formulation is commonly referred to as the factor model. There is a vast literature which focuses on using this latent factor structure for forecasting applications. A typical example is found in diffusion index models (Stock & Watson (2002b)), where latent factors are derived from a high-dimensional set of variables using Principal Components Analysis (hereafter, PCA). These factors are subsequently utilized to forecast a target variable. A limitation of this PCA-based factor estimation is its unsupervised nature, i.e. that no information from the target variable is incorporated during factor estimation.

Given that the primary goal is to forecast a target rather than estimate the underlying factor structure, introducing a degree of supervision can prove beneficial. This can help in filtering out irrelevant information from the predictor set, thus enhancing the predictive accuracy .This can be done in different ways; using soft and hard thresholding methods to remove predictors with no predictive content, as in Bai & Ng (2008), or assign varying weights to predictors based on their predictive capabilities for the target (see, for example, Huang *et al.* (2022)), or estimate the subset of factors that exhibit predictive power for the target rather than the complete set of factors that drive the target, as in Kelly & Pruitt (2015).

The aforementioned models, whether utilizing PCA or supervised factor models, are predicated on the convenient assumption of linearity. However, as underscored in Goulet Coulombe *et al.* (2022), non-linearity often characterizes many predictive relationships, particularly over extended time horizons and within data-rich environments.

Various approaches have been proposed to integrate non-linearity into factor models. For instance, squared principal components (PCs) or principal component squared (PC^2) as seen in Bai & Ng (2008), sufficient forecasting by Fan *et al.* (2017), the kernel trick to estimate factors (Kutateladze (2022)) among others. However, these approaches have limited supervision in the prediction process, if any. For example, Fan *et al.* (2017) estimates factors through an unsupervised method (PCA) and then derives sufficient indices using these PCs. Similarly, Kutateladze (2022) essentially applies kernel PCA to estimate the set of factors driving a higher-dimensional space obtained by lifting the set of predictors through the kernel method. Similarly, Bai & Ng (2008), despite employing thresholding to reduce squared PCs to a smaller set, may still encounter challenges in potentially estimating irrelevant factors within this subset, leading to inefficiency. Moreover, in Bai & Ng (2008), a very particular form of non-linearity (quadratic) is examined, which is somewhat ad hoc.

Our paper incorporates non-linearity by introducing a novel kernel three-pass regression filter. Our approach essentially applies the three-pass filter (hereafter 3PRF) proposed by Kelly & Pruitt (2015) to a transformed set of predictors. We adopt the lifting concept similar to Kutateladze (2022), but instead of employing an unsupervised method like kernel PCA, we utilize a supervised method to estimate factors relevant to the target variable. The basic idea behind our approach is that many non-linear relationships observed in one space exhibit linearity in another space.

The table below summarizes our discussion by listing some popular methods in literature and how this paper is placed among them.

Table 1: Factor Model Based Forecasting Methods

	Linear	Non-Linear
Unsupervised	PC	kernel PCA, Sq-PC, $PC - sq$
Supervised	3PRF	This Paper

The paper proceeds as follows. Section 2 provides a brief introduction to Kernel methods and lists examples of some widely used kernels. Section 3 introduces our estimator and discusses its similarity with the estimator of Kelly & Pruitt (2015). We also list a set of assumptions that ensure the theoretical properties our estimators, which are given in the subsequent section 4. We present our empirical results in sections 5 and 6 and we finally conclude in section 6. Mathematical proofs and implementation details are given in the appendix.

Definitions and notations

We use $\boldsymbol{y}$ to denote the $\mathrm{T} \times 1$ vector of the target variable, i.e. $\boldsymbol{y} = (y_h, y_{h+1} \dots y_{t+h})$. We have N predictors with T observations for each predictor. The cross section of predictors at a time t is given by the $N \times 1$ vector $\boldsymbol{x}_t$. Similarly, the vector of temporal observations of a predictor i is given by $\mathbf{x}_i$. We stack the predictors in a $T \times N$ matrix $\boldsymbol{X}$, $\boldsymbol{X} = (\boldsymbol{x}'_1, \boldsymbol{x}'_2, \dots, \boldsymbol{x}'_T)' = (\mathbf{x}_1, \mathbf{x}_2, \dots, \mathbf{x}_N)$. We have L proxies which we stack in a $T \times\ L$ matrix $\boldsymbol{Z} = (\boldsymbol{z}'_1, \boldsymbol{z}'_2, \dots, \boldsymbol{z}'_T)'$ $\boldsymbol{J}_T \equiv \boldsymbol{I}_T - \frac{1}{T}\iota_T\iota'_T$, where $\boldsymbol{I}_T$ is the T-dimensional identity matrix and ι_T the T-vector of ones. For matrices $\boldsymbol{U}$ and $\boldsymbol{V}$ of conformable dimensions, $\boldsymbol{S}_{UV} \equiv \boldsymbol{U}'\boldsymbol{J}_T\boldsymbol{V}$. For the transformed set of predictors $\varphi(\boldsymbol{X})$, $\varphi_j(\mathbf{x})$ denotes the j^{th} observation. $\varphi(\boldsymbol{X}) = (\varphi_1(\mathbf{x}), \varphi_2(\mathbf{x}), \dots, \varphi_M(\mathbf{x})) = (\varphi(\boldsymbol{x}_1)', \varphi(\boldsymbol{x}_2)', \dots, \varphi(\boldsymbol{x}_T)')'$ Stochastic orders are denoted by the usual O_p and o_p. For a matrix, $\boldsymbol{O}_p$ and $\boldsymbol{o}_p$ denotes the element wise stochastic order, i.e., a matrix is said to be $\boldsymbol{O}_p(1)$ or $\boldsymbol{o}_p(1)$ if all it's elements are $O_p(1)$ or $o_p(1)$ respectively.

2 Kernel Method

The kernel method uses an implicit mapping of the data (X) space into a higher-dimensional space[1] $(\mathcal{F})$, which contains non-linear transformations of the given data. We denote this transformation by $\varphi : X \to \mathcal{F}$. This transformation offers a significant advantage since many non-linear relationships can be reformulated as linear relationships in an appropriately transformed space. Transformation to a higher-dimensional space using the kernel method makes

[1] This higher dimensional space is Hilbert space where the inner product of the vectors is well defined.

a large set of non-linear forms available, rendering the discovery of a nonlinear relationship very likely. To illustrate how a nonlinear relation can be reformulated as a linear relation with appropriately transformed variables, consider the following example. We generate 2 variables X and Y from uniform distribution $U[-2, 2]$. Define a binary variable z as:

$$z = \begin{cases} 1 & \text{if } X^2 + Y^2 \leq 2 \\ -1 & \text{otherwise} \end{cases}$$

It proves challenging if we attempt to use a linear boundary to separate the two classes of variable z. However, upon transforming the original spaces X and Y to $\varphi_1(X) = \sin^2(X)$ and $\varphi_2(Y) = \cos^2(Y)$ respectively, we find that the two classes can be easily distinguished as seen in figure-1. The blue points are in class 1, and the red ones are in class -1. Note that on

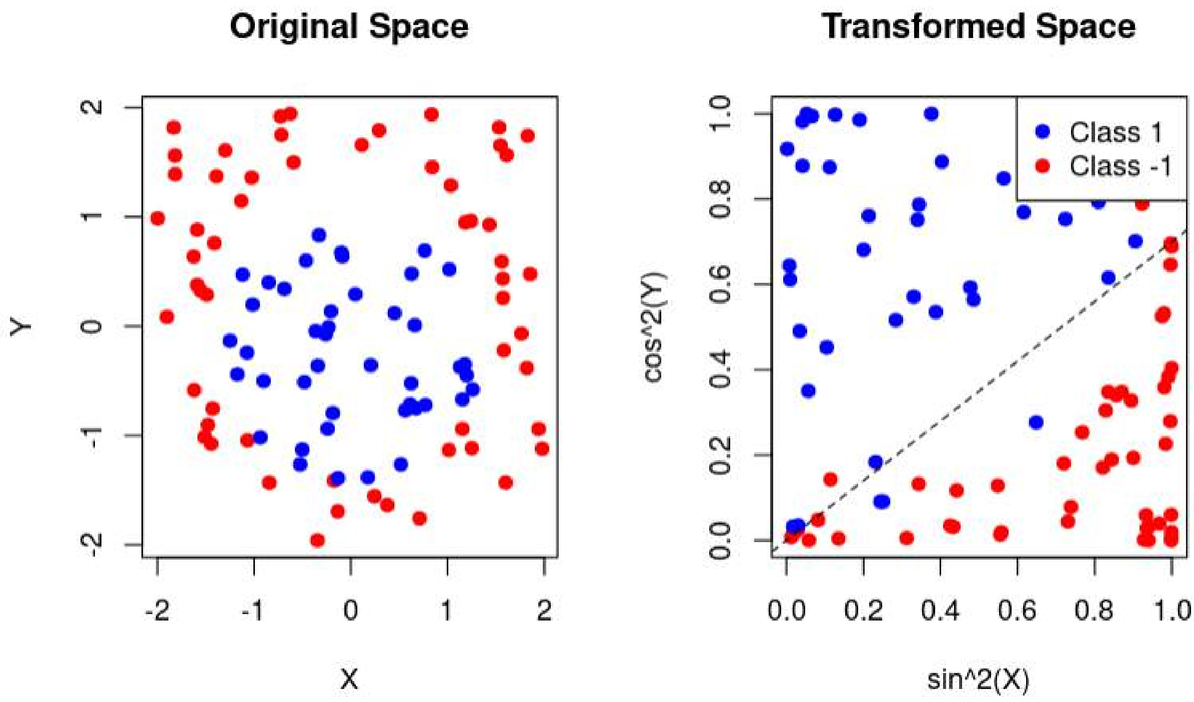

Figure 1: Non-Linear Transformation Making Classification Easy

the left-hand side, no line can achieve a decent accuracy in classification in the original space.

However, we can easily do so in the transformed space on the right.

For the sake of simplicity, this example illustrates the transformation of a two-dimensional input (X, Y) into a two-dimensional feature space. However, the transformed space $\varphi(X)$ is typically high-dimensional and potentially infinite-dimensional. As the dimensions of the transformed space grow, it captures the non-linearity better by virtue of the presence of more non-linear transformations of the input data. But this high (infinite)-dimensionality of transformed space seemingly makes computations extremely challenging (infeasible). The kernel method provides a solution to this issue. Our problem necessitates the computation of the similarity measure between transformed data points $\varphi(x_i)$ and $\varphi(x_j)$ via the inner product $\varphi(x_i)'\varphi(x_j)$, which appears to require knowledge of the function $\varphi(\cdot)$. The kernel function $\mathcal{K}(\cdot,\cdot) : X \times X \to R$ circumvents this requirement by computing the aforementioned similarity measure without necessitating knowledge of the feature map $\varphi(\cdot)$. Mercer's condition ensures the existence of a feature map $\varphi(\cdot)$ for a valid (positive definite) kernel function in Hilbert space. A detailed discussion of Mercer's condition can be found in Appendix - A.2. In the remaining part of this section, we illustrate how the kernel function computes the inner products by showing an explicit functional form of $\varphi(\cdot)$.

Some Popular Kernel Methods and Their Working

Many popular kernel functions exist, such as polynomial, Gaussian, and sigmoid kernels. We illustrate two of them to show that kernel function can represent the products of feature map $\varphi(\cdot)$.

Polynomial Kernel Let the functional mapping where $\varphi(a)$ includes a fixed term, all variables $a_1, a_2, \ldots, a_N$, and their respective squares and cross products. The kernel function $\mathcal{K}(a, b)$ assumes a simplified structure if we scale the linear and cross-product terms in $\varphi(a)$ by the constant $\sqrt{2}$. In other words, if we define

$$\varphi(a) = \Big(1, \sqrt{2}a_1, \sqrt{2}a_2, \ldots, \sqrt{2}a_N, a_1^2, a_2^2, \\ \ldots, a_N^2, \sqrt{2}a_1a_2, \sqrt{2}a_1a_3, \ldots, \sqrt{2}a_{N-1}a_N\Big)',$$

Then, the corresponding kernel function becomes:

$$\begin{aligned}
\mathcal{K}(a,b) =& \varphi(a)'\varphi(b) \\
=& 1 + 2\left(a_1b_1 + a_2b_2 + \cdots + a_Nb_N\right) + \left(a_1^2b_1^2 + a_2^2b_2^2 + \cdots + a_N^2b_N^2\right) \\
&+ 2\left(a_1a_2b_1b_2 + a_1a_3b_1b_3 + \cdots + a_{N-1}a_Nb_{N-1}b_N\right) \\
=& 1 + 2\left(a_1b_1 + a_2b_2 + \cdots + a_Nb_N\right) + \left(a_1b_1 + a_2b_2 + \cdots + a_Nb_N\right)^2 \\
=& 1 + 2a'b + \left(a'b\right)^2 = \left(1 + a'b\right)^2
\end{aligned}$$

This kernel can be generalized to a general degree d by keeping the terms of degree at most d in the expression of $\varphi(a)$. This example is also discussed in Exterkate *et al.* (2016).

Gaussian Kernel This kernel goes beyond the high-dimensional kernel. This kernel is, in fact, infinite-dimensional. Let $\mathrm{x}, \mathrm{z} \in \mathbb{R}^k$ and $\mathcal{K}(\mathrm{x},\mathrm{z}) = e^{-\gamma\|\mathrm{x}-\mathrm{z}\|^2}$. Then, through the Taylor expansion, we can write

$$\begin{aligned}
\mathcal{K}(\mathrm{x},\mathrm{z}) =& e^{-\gamma\|\mathrm{x}\|^2}e^{-\gamma\|z\|^2}e^{2\gamma\mathrm{x}'z} = e^{-\gamma\|\mathrm{x}\|^2}e^{-\gamma\|z\|^2}\sum_{j=0}^{\infty}\frac{(2\gamma)^j}{j!}\left(\mathrm{x}'\mathrm{z}\right)^j \\
=& e^{-\gamma\|\mathrm{x}\|^2}e^{-\gamma\|z\|^2}\sum_{j=0}^{\infty}\frac{(2\gamma)^j}{j!}\sum_{\sum_{i=1}^k n_i=j} j!\prod_{i=1}^k\frac{(x_iy_i)^{n_i}}{n_i!} \\
=& \sum_{j=0}^{\infty}\sum_{\sum_{i=1}^k n_i=j}\left((2\gamma)^{j/2}e^{-\gamma\|x\|^2}\prod_{i=1}^k\frac{x_i^{n_i}}{\sqrt{n_i!}}\right)\times\left((2\gamma)^{j/2}e^{-\gamma\|z\|^2}\prod_{i=1}^k\frac{y_i^{n_i}}{n_i!}\right) \\
=& \varphi(\mathrm{x})'\varphi(\mathrm{z})
\end{aligned}$$

That is, $\varphi_j(\mathrm{x}) = \sum_{\sum_{i=1}^k n_i=j}(2\gamma)^{j/2}e^{-\gamma\|\mathrm{x}\|^2}\prod_{i=1}^k\frac{x_i^{n_i}}{\sqrt{n_i!}}, \quad j = 0, \ldots, \infty.$ Kutateladze (2022) use this kernel function in their paper which is based on kernel PCA.

3 The Estimator

We delineate the three regression passes that we use to construct our forecast. The first two passes, as explained below, are not feasible in practice, whilst the eventual closed-form solutions are. Nonetheless, these steps offer valuable insights into the underlying process of our estimator and elucidate its similarity to the well-known linear three-pass filter proposed by Kelly & Pruitt (2015).

Below, we list the data generation process for the transformed predictor set ($\varphi(\boldsymbol{x}_t)$), the target ($\boldsymbol{y}$), and the proxies employed for supervision ($\boldsymbol{Z}$). Given the data structure, it is easy to explain why this supervised methodology is effective in estimating the target relevant factors.

Assumption 1 *Data generating Process.*

$$\varphi(\boldsymbol{x}_t) = \boldsymbol{\Phi}\boldsymbol{F}_t + \boldsymbol{\varepsilon}_t \qquad y_{t+h} = \beta_0 + \boldsymbol{\beta}'\boldsymbol{F}_t + \eta_{t+h} \qquad \boldsymbol{z}_t = \boldsymbol{\lambda}_0 + \boldsymbol{\Lambda}\boldsymbol{F}_t + \boldsymbol{\omega}_t$$

$$\varphi(\boldsymbol{X}) = \boldsymbol{F}\boldsymbol{\Phi}' + \boldsymbol{\varepsilon} \qquad \boldsymbol{y} = \boldsymbol{\iota}_T\beta_0 + \boldsymbol{F}\boldsymbol{\beta} + \boldsymbol{\eta} \qquad \boldsymbol{Z} = \boldsymbol{\iota}_T\boldsymbol{\lambda}_0' + \boldsymbol{F}\boldsymbol{\Lambda}' + \boldsymbol{\omega}$$

where $\boldsymbol{F}_t = \left(\boldsymbol{f}_t', \boldsymbol{g}_t'\right)'$, $\boldsymbol{\Phi} = \left(\boldsymbol{\Phi}_f, \boldsymbol{\Phi}_g\right)$, $\boldsymbol{\Lambda} = (\boldsymbol{\Lambda}_f, \boldsymbol{\Lambda}_g)$, *and* $\boldsymbol{\beta} = \left(\boldsymbol{\beta}_f', \boldsymbol{0}'\right)'$ *with* $\left|\boldsymbol{\beta}_f\right| > \boldsymbol{0}$. $K_f > 0$ *is the dimension of vector* $\boldsymbol{f}_t, K_g \geq 0$ *is the dimension of vector* $\boldsymbol{g}_t, L > 0$ *is the dimension of vector* $\boldsymbol{z}_t$, *and* $K = K_f + K_g$.

φ maps our N-dimensional predictors $\boldsymbol{x}_t$ to a higher M-dimensional space. Assumption 1 endows this transformed set of predictors with a factor structure. An underlying factor structure among $\boldsymbol{X}$ implies the existence of a low dimensional plane, projection onto which explains maximal variation in the predictors. An equivalent interpretation of a linear factor structure on $\varphi(\boldsymbol{x}_t)$ would be the existence of a lower dimensional manifold which explains maximum variation in $\boldsymbol{x}_t$. The basis of this manifold is comprised of a few uni-dimensional orthogonal projections of $\varphi(\boldsymbol{x}_t)$.

At this juncture, it's instructive to discuss the difference between our methodology and a set of non-linear dimension reduction methods categorized under the umbrella term 'Sufficient Dimension Reduction (SDR)'. Sufficient dimension reduction techniques hinge upon the existence of a central subspace for $\boldsymbol{X}$, such that for every t, $y_{t+h} \perp \boldsymbol{x}_t | H^T \boldsymbol{x}_t$, where H is an $N \times L$ matrix with $L << N$, is a small fixed number. Matrix H projects $\boldsymbol{x}_t$ onto an L-dimensional subspace, termed the central subspace. This projection is deemed 'sufficient' for predicting y_{t+h}, indicating that $\boldsymbol{x}_t - H^T \boldsymbol{x}_t$ is redundant from the perspective of predicting y_{t+h}. SDR accommodates non-linearity by permitting y_{t+h} to be a non-linear function (called the link function) of $H^T \boldsymbol{x}_t$, i.e. SDR posits that

$$y_{t+h} = f(H^T \boldsymbol{x}_t) \text{ for some unknown function } f$$

For more details, see Cook (2018) and Li (2018).

In contrast, our framework posits the existence of a lower-dimensional manifold of $\boldsymbol{x}_t$, equivalently a subspace of $\varphi(\boldsymbol{x}_t)$ [2] such that y_{t+h} is 'linearly' independent of $\varphi(\boldsymbol{x}_t)$, conditioning on $H_2^T \varphi(\boldsymbol{x}_t)$[3], where the columns of $H_2^T \varphi(\boldsymbol{x}_t)$ constitutes an ortho-normal basis for that lower-dimensional subspace. Therefore, the projection of $\varphi(\boldsymbol{x}_t)$ onto H_2 is adequate to characterize any linear dependence of $\boldsymbol{y}$ on $\varphi(\boldsymbol{X})$. Non-linearity, in our setup, unlike SDR, is accommodated through this projection of the transformed set of predictors[4], not through a non-linear link function.

We now delineate the infeasible three-passes below.

[2] φ denotes a suitable transformation

[3] H_2 is a $M \times k$ matrix and $K << M$

[4] Lower dimensional subspace of the transformed set of predictors is equivalent to a non-linear manifold of the original predictors

Stage-1	
Pass	Description
1.	Run time series regression of $\varphi_j(\mathbf{x})$ on $\boldsymbol{Z}$ for $j = 1, \ldots, M$, $\varphi_j(\boldsymbol{x}_t) = \tilde{\phi}_{0,j} + \boldsymbol{z}_t' \tilde{\boldsymbol{\phi}}_j + \hat{v}_{1jt}$, retain slope estimate $\tilde{\boldsymbol{\phi}}_j$.
2.	Run cross section regression of $\varphi(\boldsymbol{x}_t)$ on $\tilde{\boldsymbol{\phi}}$ for $t = 1, \ldots, T$, $\varphi_j(\boldsymbol{x}_t) = \tilde{\boldsymbol{\phi}}_j' \hat{\boldsymbol{F}}_t + \hat{v}_{2jt}$, retain slope estimate $\hat{\boldsymbol{F}}_t$.
3.	Run time series regression of y_{t+h} on predictive factors $\hat{\boldsymbol{F}}_t$, $\hat{y}_{t+h} = \hat{\beta}_0 + \hat{\boldsymbol{F}}' \hat{\boldsymbol{\beta}}$, delivers the forecast.

Table 2: Kernel 3PRF

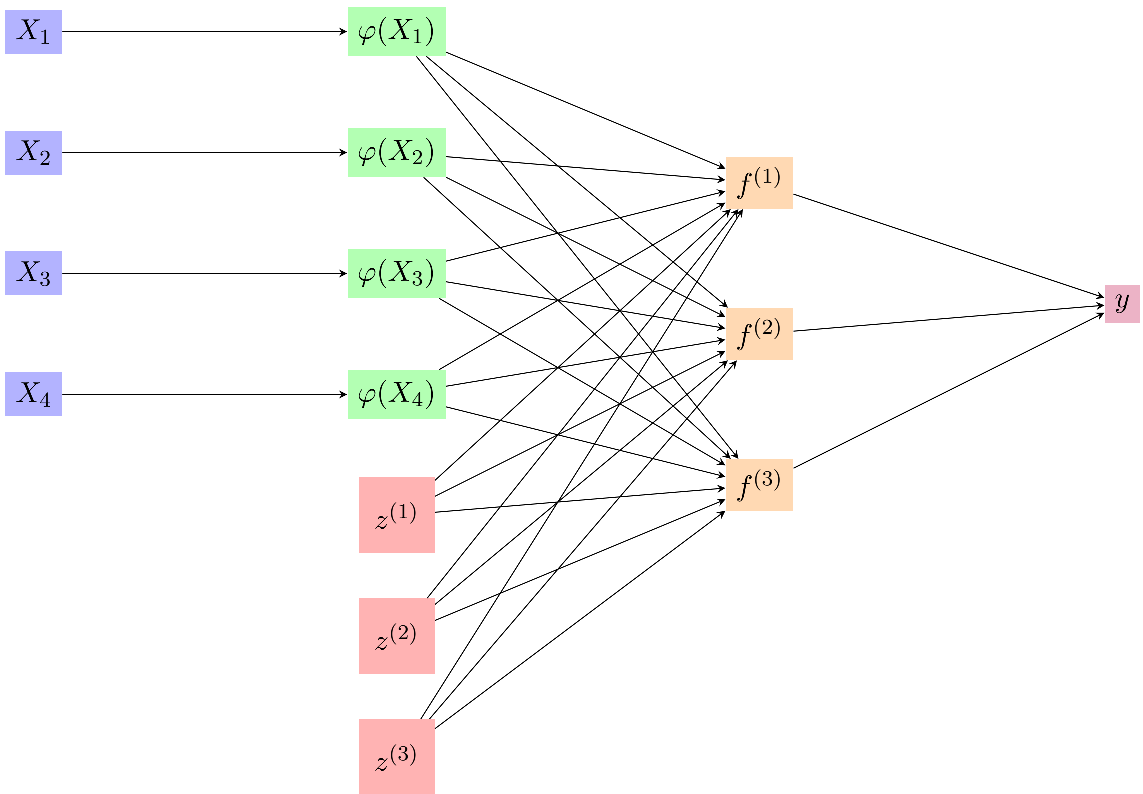

Figure 2: Implementation of the Three Pass regression filter for the case T=4 and L=3 relevant factors. The variables $z^{(1)} \ldots z^{(3)}$ and $f^{(1)} \ldots f^{(3)}$ are the vectors representing the time series of the respective variables. X_s, (resp $\varphi(X_s)$) represents the cross section of $\boldsymbol{X}$ (resp $\varphi(\boldsymbol{X})$) in period s.

These three passes rely on the fact that the correlation between the transformed $\varphi(\boldsymbol{X})$ and the proxies is only due to target relevant factors. Therefore, pass 1 of the regression asymptotically yields a rotation of the relevant-factor loadings of the j^{th} predictor. Cross sectional covariance between these loadings and the predictors, across t, is solely affected by the target relevant factor(s). Hence, pass 2 of this process traces the factor(s) out as a slope parameter. Although these three passes offer valuable insights into the mechanics of our process, they are infeasible in practise due to the unavailability of the transformed inputs $\varphi(\boldsymbol{X})$. This is where, the kernel trick shall prove to be handy. To see this, we note that factor(s), their predictive coefficients and the forecast can be expressed in closed form as below,
The estimated factor(s) :

$$\begin{aligned}
\hat{\boldsymbol{F}}' &= \boldsymbol{S}_{ZZ}\left(\boldsymbol{S}'_{\varphi(X)Z}\boldsymbol{S}_{\varphi(X)Z}\right)^{-1}\boldsymbol{S}'_{\varphi(X)Z}\varphi(\boldsymbol{X})' \\
&= \boldsymbol{Z}'\boldsymbol{J}_T\boldsymbol{Z}\left(\boldsymbol{Z}'\boldsymbol{J}_T\varphi(\boldsymbol{X})\varphi(\boldsymbol{X})'\boldsymbol{J}_T\boldsymbol{Z}\right)^{-1}\boldsymbol{Z}'\boldsymbol{J}_T\varphi(\boldsymbol{X})\varphi(\boldsymbol{X})' \\
&= \boldsymbol{Z}'\boldsymbol{J}_T\boldsymbol{Z}\left(\boldsymbol{Z}'\boldsymbol{J}_T\mathcal{K}(\boldsymbol{X},\boldsymbol{X}')\boldsymbol{J}_T\boldsymbol{Z}\right)^{-1}\boldsymbol{Z}'\boldsymbol{J}_T\mathcal{K}(\boldsymbol{X},\boldsymbol{X}')
\end{aligned}$$

The estimated coefficient(s) of the factor(s) :

$$\begin{aligned}
\hat{\boldsymbol{\beta}} &= \boldsymbol{S}_{ZZ}\boldsymbol{S}_{\varphi(\boldsymbol{X})Z}\boldsymbol{S}_{\varphi(\boldsymbol{X})Z}\left(\boldsymbol{S}'_{\varphi(\boldsymbol{X})Z}\boldsymbol{S}_{\varphi(\boldsymbol{X})\varphi(\boldsymbol{X})}\boldsymbol{S}_{\varphi(\boldsymbol{X})Z}\right)^{-1}\boldsymbol{S}'_{\varphi(\boldsymbol{X})Z}\boldsymbol{S}_{\varphi(\boldsymbol{X})y}. \\
&= \left(\boldsymbol{Z}'\boldsymbol{J}_T\boldsymbol{Z}\right)^{-1}\boldsymbol{Z}'\boldsymbol{J}_T\varphi(\boldsymbol{X})\varphi(\boldsymbol{X})'\boldsymbol{J}_T\boldsymbol{Z}\left(\boldsymbol{Z}'\boldsymbol{J}_T\varphi(\boldsymbol{X})\varphi(\boldsymbol{X})'\boldsymbol{J}_T\varphi(\boldsymbol{X})\varphi(\boldsymbol{X})'\boldsymbol{J}_T\boldsymbol{Z}\right)^{-1}\boldsymbol{Z}'\boldsymbol{J}_T\varphi(\boldsymbol{X})\varphi(\boldsymbol{X})'\boldsymbol{J}_T\boldsymbol{y} \\
&= \left(\boldsymbol{Z}'\boldsymbol{J}_T\boldsymbol{Z}\right)^{-1}\boldsymbol{Z}'\boldsymbol{J}_T\mathcal{K}(\boldsymbol{X},\boldsymbol{X}')\boldsymbol{J}_T\boldsymbol{Z}\left(\boldsymbol{Z}'\boldsymbol{J}_T\mathcal{K}(\boldsymbol{X},\boldsymbol{X}')\boldsymbol{J}_T\mathcal{K}(\boldsymbol{X},\boldsymbol{X}')\boldsymbol{J}_T\boldsymbol{Z}\right)^{-1}\boldsymbol{Z}'\boldsymbol{J}_T\mathcal{K}(\boldsymbol{X},\boldsymbol{X}')\boldsymbol{J}_T\boldsymbol{y}
\end{aligned}$$

Finally, the estimated target :

$$
\begin{aligned}
\hat{\boldsymbol{y}} &= \iota_T \bar{y} + \boldsymbol{J}_T \hat{\boldsymbol{F}} \hat{\boldsymbol{\beta}} \\
&= \iota_T \bar{y} + \boldsymbol{J}_T \varphi(\boldsymbol{X}) \boldsymbol{S}_{\varphi(\boldsymbol{X})Z} \left(\boldsymbol{S}'_{\varphi(\boldsymbol{X})Z} \boldsymbol{S}_{\varphi(\boldsymbol{X})\varphi(\boldsymbol{X})} \boldsymbol{S}_{\varphi(\boldsymbol{X})\varphi(\boldsymbol{X})} \right)^{-1} \boldsymbol{S}'_{\varphi(\boldsymbol{X})Z} \boldsymbol{S}_{\varphi(\boldsymbol{X})y} \\
&= \iota \bar{y} + \boldsymbol{J}_T \varphi(\boldsymbol{X}) \varphi(\boldsymbol{X})' \boldsymbol{J}_T \boldsymbol{Z} \left(\boldsymbol{Z}' \boldsymbol{J}_T \varphi(\boldsymbol{X}) \varphi(\boldsymbol{X})' \boldsymbol{J}_T \varphi(\boldsymbol{X}) \varphi(\boldsymbol{X})' \boldsymbol{J}_T \boldsymbol{Z} \right)^{-1} \boldsymbol{Z}' \boldsymbol{J}_T \varphi(\boldsymbol{X}) \varphi(\boldsymbol{X})' \boldsymbol{J}_T \boldsymbol{y} \\
&= \iota \bar{y} + \boldsymbol{J}_T \mathcal{K}(\boldsymbol{X}, \boldsymbol{X}') \boldsymbol{J}_T \boldsymbol{Z} \left(\boldsymbol{Z}' \boldsymbol{J}_T \mathcal{K}(\boldsymbol{X}, \boldsymbol{X}') \boldsymbol{J}_T \mathcal{K}(\boldsymbol{X}, \boldsymbol{X}') \boldsymbol{J}_T \boldsymbol{Z} \right)^{-1} \boldsymbol{Z}' \boldsymbol{J}_T \mathcal{K}(\boldsymbol{X}, \boldsymbol{X}') \boldsymbol{J}_T \boldsymbol{y}
\end{aligned}
$$

These are obtained by simply replacing $\boldsymbol{X}$ by $\varphi(\boldsymbol{X})$ in the three-pass regression filter of Kelly & Pruitt (2015). As evident from the expression of $\hat{\boldsymbol{F}}'$, our three-pass filter applied on the transformed predictor space results in a favorable scenario where the eventual estimate of the factor(s) depends upon the transformed predictors only through their dot products in the transformed space. This holds true for $\hat{\boldsymbol{\beta}}$ and $\hat{\boldsymbol{y}}$ as well.

This inner product can be computed using a suitable kernel function. Alternatively, it can be inferred that employing a positive semidefinite (psd) kernel function to calculate dot products in these derived expressions is akin to executing the three-pass filter process on the implied transformed space, which, according to Mercer's theorem, is guaranteed to exist.

The Kernel three-pass regression, just like the linear 3PRF, relies on the availability of suitable proxies. Kelly & Pruitt (2015) shows that such proxies can always be constructed using the target variable $\boldsymbol{y}$. That process is explained below.

0.	Initialize $\boldsymbol{r}_0 = \boldsymbol{y}$. For $k = 1, \ldots, L$. (L is the total number of proxies)
1.	Define the k^{th} automatic proxy to be $\boldsymbol{r}_{k-1}$. Stop if $k = L$; otherwise proceed.
2.	Compute the k3PRF for target $\boldsymbol{y}$ using cross-section $\boldsymbol{X}$ using statistical proxies 1 through k. Denote the resulting forecast $\hat{\boldsymbol{y}}_k$.
3.	Calculate $\boldsymbol{r}_k = \boldsymbol{y} - \hat{\boldsymbol{y}}_k$, advance k, and go to step 1.

Table 3: Automatic Proxy-Selection Algorithm

Assumption 1 lays out the factor structure of our model. Below, we delineate a set of additional assumptions under which our model delivers consistent forecasts.

Assumption 2 *(Factors, Loadings and Residuals).*

Let $R < \infty$. For any i, s, t and some $0 < \psi \leq 1$,

1. $\mathbb{E}\left\|\boldsymbol{F}_t\right\|^4 < R, T^{-1} \sum_{s=1}^{T} \boldsymbol{F}_s \xrightarrow[T\to\infty]{p} \boldsymbol{\mu}$ *and* $T^{-1/2}\left(\boldsymbol{F}'\boldsymbol{J}_T\boldsymbol{F} - \boldsymbol{\Delta}_F\right) = \boldsymbol{O}_p(1)$.
2. $\mathbb{E}\left\|\phi_i\right\|^4 \leq R, M^{-1} \sum_{j=1}^{N} \phi_j \xrightarrow[N\to\infty]{p} \mathbf{0}$, $M^{-1/2}\left(\boldsymbol{\Phi}'\boldsymbol{\Phi} - \mathcal{P}\right) = \boldsymbol{O}_p(1)$.
3. $\mathbb{E}\left(\varepsilon_{it}\right) = 0, \mathbb{E}\left|\varepsilon_{it}\right|^8 \leq R$
4. $\mathbb{E}\left(\boldsymbol{\omega}_t\right) = \mathbf{0}, \mathbb{E}\left\|\boldsymbol{\omega}_t\right\|^4 \leq R, T^{-1/2} \sum_{s=1}^{T} \boldsymbol{\omega}_s = \boldsymbol{O}_p(1)$ *and* $T^{-1}\boldsymbol{\omega}'\boldsymbol{J}_T\boldsymbol{\omega} \xrightarrow[N\to\infty]{p} \boldsymbol{\Delta}_\omega$
5. $\mathbb{E}_t\left(\eta_{t+h}\right) = \mathbb{E}\left(\eta_{t+h} \mid y_t, F_t, y_{t-1}, F_{t-1}, \ldots\right) = 0, \mathbb{E}\left(\eta_{t+h}^2\right) = \delta_\eta < \infty$, *and* η_{t+h} *is independent of* $\phi_i(m)$ *and* $\varepsilon_{i,t}$ *for any* $h > 0$.

Assumption 2.1 requires that our factors are regular in the sense that their covariance matrix is well-behaved asymptotically. Assumption 2.2 is an adaptation from Kelly & Pruitt (2015). Since we assume a factor structure on the transformed space instead of the original predictor space, the normalization in various terms features M and not N, where M is the dimension of our transformed space. Assumptions 2.3-2.5 borrowed from Kelly & Pruitt (2015), impose regularity on various error processes.

Assumption 3 *(Dependence).*

Let $x(m)$ denote the m^{th} element of $\boldsymbol{x}$. For $R < \infty$ and any i, j, t, s, m_1, m_2

1. $\mathbb{E}\left(\varepsilon_{it}\varepsilon_{js}\right) = \sigma_{ij,ts}, \left|\sigma_{ij,ts}\right| \leq \bar{\sigma}_{ij}$ *and* $\left|\sigma_{ij,ts}\right| \leq \tau_{ts}$, *and*
   - a. $M^{-1} \sum_{i,j=1}^{N} \bar{\sigma}_{ij} \leq R$
   - b. $T^{-1} \sum_{t,s=1}^{T} \tau_{ts} \leq R$
   - c. $M^{-1} \sum_{i,s} \left|\sigma_{ii,ts}\right| \leq R$
   - d. $M^{-1}T^{-1} \sum_{i,j,t,s} \left|\sigma_{ij,ts}\right| \leq R$
2. $\mathbb{E}\left|M^{-1/2}T^{-1/2} \sum_{s=1}^{T} \sum_{i=1}^{N} \left[\varepsilon_{is}\varepsilon_{it} - \sigma_{ii,st}\right]\right|^4 \leq R$
3. $\mathbb{E}\left|T^{-1/2} \sum_{t=1}^{T} F_t\left(m_1\right) \omega_t\left(m_2\right)\right|^2 \leq R$

4. $\mathbb{E}\left|T^{-1/2}\sum_{t=1}^{T}\omega_t\left(m_1\right)\varepsilon_{it}\right|^2 \leq R.$

5. $\mathbb{E}\left|T^{-1/2}\sum_{t=1}^{T}F_t\left(m_1\right)\varepsilon_{it}\right|^2 \leq R$

6. $\mathbb{E}\left|M^{-1/2}\sum_{i=1}^{M}\phi_i\left(m_1\right)\varepsilon_{it}\right|^2 \leq R.$

7. $\mathbb{E}\left|T^{-1/2}\sum_{t=1}^{T}F_t\left(m_1\right)\eta_{t+h}\right|^2 \leq R$

Assumption 3.1-3.2 allow various forms of weak cross-sectional and temporal dependence between the idiosyncratic components of the transformed predictors. These assumptions characterize our 'Approximate' factor model. The terminology of approximate, as opposed to a strict factor model, alludes to the allowance of these weak correlations, as outlined by Chamberlain & Rothschild (1983). These assumptions are standard in the literature; see Bai (2003). Assumption 3.4-3.7 are either borrowed from or are weaker versions of Assumptions in Kelly & Pruitt (2015). They are reasonable because each of them involves a product of orthogonal series.

Assumption 4 *(Normalization).*

1. $\mathcal{P} = \boldsymbol{I}$

2. $\boldsymbol{\Delta}_F$ *is diagonal, positive definite, and each diagonal element is unique and bounded.*

Assumption 4 is a normalization assumption that is common in factor model literature. It pertains to the non-identifiability of the true factor(s). It is well known that only the vector space spanned by the factor(s) can be consistently estimated but not the factor themselves. Imposing some normalization condition for the uniqueness of solution(s) is common in literature.

Assumption 5 *(Relevant Proxies).*

1. $\boldsymbol{\Lambda} = \begin{bmatrix} \boldsymbol{\Lambda}_f & \mathbf{0} \end{bmatrix}$

2. $\mathbf{\Lambda}_f$ *is non-singular.*

5 outlines the utility of using proxies. Proxies are target-relevant in the sense that they only load on the factor(s) that have any explanatory power for the target. Non-singularity of $\mathbf{\Lambda}_f$ ensures that none of the proxies are redundant.

4 Results

We show that our estimated forecast converges to the infeasible best in probability. To show the same, we prove some intermediate results. All the proofs are in the appendix.

Define $\delta_{MT} \equiv min\{\sqrt{M}, \sqrt{T}\}$. Define $\boldsymbol{H}_f \equiv \hat{\boldsymbol{F}}_A \hat{\boldsymbol{F}}_B^{-1} \mathbf{\Lambda} \mathbf{\Delta}_F \mathcal{P}$ where, $\hat{\boldsymbol{F}}_A = T^{-1}\boldsymbol{Z}'\boldsymbol{J}_T\boldsymbol{Z}$ and $\hat{\boldsymbol{F}}_B = M^{-1}T^{-2}\boldsymbol{Z}'\boldsymbol{J}_T\varphi(\boldsymbol{X})\varphi(\boldsymbol{X}')\boldsymbol{J}_T\boldsymbol{Z}$

Theorem 1 *If Assumption 1-5 hold, we have*

$$\hat{\boldsymbol{F}}_t - \boldsymbol{H}_f \boldsymbol{f}_t = \boldsymbol{O}_p(\delta_{MT}^{-1})$$

This theorem establishes the estimated factor(s) convergence to the true factors up to a rotation. It is well known in the literature on factor models[5], that true underlying factor(s) are not identifiable; we instead estimate a rotated version of the true factors, which preserves their span.

Define $\boldsymbol{G}_\beta \equiv \hat{\boldsymbol{\beta}}_1^{-1} \hat{\boldsymbol{\beta}}_2 \left[\mathbf{\Lambda}\mathbf{\Delta}_F\mathcal{P}\mathbf{\Delta}_F\mathcal{P}\mathbf{\Delta}_F\mathbf{\Lambda}'\right]^{-1} \mathbf{\Lambda}\mathbf{\Delta}_F\mathcal{P}\mathbf{\Delta}_F$, where
$\hat{\boldsymbol{\beta}}_1 = \hat{\boldsymbol{F}}_A$ and $\hat{\boldsymbol{\beta}}_2 = \hat{\boldsymbol{F}}_B$

[5] This feature of inherent unidentifiability has been emphasized in Bai (2003), Kelly & Pruitt (2015) among other papers. The normalization imposed in assumption 5 is done to handle this issue.

Theorem 2 *If Assumption 1-5 hold, we have*

$$\hat{\boldsymbol{\beta}} - \boldsymbol{G}_{\beta}\boldsymbol{\beta} = \boldsymbol{O}_p(\delta_{MT}^{-1}).$$

$\boldsymbol{H}_f{}'\boldsymbol{G}_{\beta} = \boldsymbol{I}$

This theorem establishes the convergence of the predictive coefficients to a rotation of the true coefficients. Just like in the case of factor(s), true coefficients are not identifiable and we instead estimate their rotation. The rates established in **Theorems** 1 and 2 differ from the rates established in Kelly & Pruitt (2015) and the reason is that our definition of rotation matrices $\boldsymbol{H}_f$ and $\boldsymbol{G}_{\beta}$ are different from Kelly & Pruitt (2015). (See Remark 1).

Remark 1 *As highlighted in Bai & Ng (2006) and also emphasized in Kelly & Pruitt (2015), the presence of matrices $\boldsymbol{H}_f$ and $\boldsymbol{G}_{\beta}$ in **Theorem** 1 and 2 highlight the fact we are essentially estimating a vector space. These theorems "pertain to the difference between $\left[\hat{\boldsymbol{F}}_t/\hat{\boldsymbol{\beta}}\right]$ and the space spanned by $[\boldsymbol{F}_t/\boldsymbol{\beta}]$". The product $\boldsymbol{H}_f'\boldsymbol{G}_{\beta}$ equals an identity matrix, cancelling the rotations in the estimated coefficients and the factors; thereby consistently estimating direction spanned by $\boldsymbol{\beta}'\boldsymbol{F}_t$. However, this characteristic is absent in Theorems 5 and 6 of Kelly & Pruitt (2015). The matrices $\boldsymbol{H}$ and $\boldsymbol{G}_{\beta}$ as defined in their paper do not necessarily yield a product that equals an identity matrix.*

Theorem 3 *If Assumption 1-5 hold, we have*

$$\hat{y}_{t+h} - \mathbb{E}_t y_{t+h} = O_p(\delta_{MT}^{-1})$$

Combining **Theorem** 1 and 2, the convergence $\hat{y}_{t+h}$ of follows directly. Our proof, unlike Kelly & Pruitt (2015) uses the convergence results for the estimated factor(s) and coefficients to obtain this result.

Remark 2 *The rates established in **Theorem** 1, 2 and 3 are different from the result in Kelly*

& Pruitt (2015) where the corresponding rates are $O_p(T^{-1/2})$, $O_p(T^{-1/2})$ and $O_p(N^{-1/2})$[6] *respectively (see **Theorems** 4, 5 and 6 in their paper). For **Theorem** 1 and 2, the difference is explained by a different definition of the rotation matrices in our paper (see **Remark** 1). For establishing the convergence of $\hat{y}_{t+h}$, their proof follows two steps. First they show that $\hat{y}_{t+h} - \tilde{y}_{t+h} = O_p(T^{-1/2})$, where $\tilde{y}_{t+h}$ is defined in their appendix. Then then they argue that $\sqrt{T}\tilde{y}_{t+h} \underset{T,N\to\infty}{\longrightarrow} \mathbb{E}_t y_{t+h}$. Since $\tilde{y}_{t+h}$*[7] *is $O_p(1)$, $\sqrt{T}\tilde{y}_{t+h}$ would diverge to infinity and their statement would be false. We presume that they erroneously wrote this and instead wanted to imply that $\sqrt{T}\left(\tilde{y}_{t+h} - \mathbb{E}_t y_{t+h}\right) \underset{T,N\to\infty}{\longrightarrow} 0$. However this statement is false because $\tilde{y}_{t+h} - \mathbb{E}_t y_{t+h}$ has random elements which converge to 0 at a rate which is $O_p(M^{-1/2}) + O_p(T^{-1/2}) = O_p(\delta_{MT}^{-1})$.*

5 Empirical Applications

In this section, we apply our proposed method to real-world applications, focusing on forecasting time series variables across various economic domains such as macroeconomics, finance, labor, housing, and prices. To assess the performance of our approach, we conduct comparative analyses against competitive methods, employing the out-of-sample R^2 performance metric as a benchmark. Additionally, we provide detailed explanations of our data, including the transformations applied to ensure stationarity and the optimization of hyperparameters related to kernel functions.

We compare our method against six different forecasting methods. The first is the PCA-based factor model proposed by Stock & Watson (2002b); we write it as *PCA* in our performance tables. Following on PCA-based methods, we compare against *PC-Squared* (*PC-Sq*) and *Squared-PC*(*Sq-PC*) of Bai & Ng (2008). The fourth method is the kernel-based PCA (*kPCA*) method implemented in Kutateladze (2022). The fifth is our linear counterpart, the *3PRF*. The last is an autoregressive model of lag order two. Some of these methods require

[6] For our case, it should have been $O_p(M^{-1/2})$ as per their theorem since we apply 3PRF to the transformed M-dimesnional space.

[7] The definition of $\tilde{y}_{t+h}$ and fact that it is $O_p(1)$ can be seen from the proof of **Theorem** 6 of Kelly & Pruitt (2015)

tuning of hyper-parameters to provide the best results, we do tune them as discussed in the subsection-5.2. Further, kernel method-based papers report results with different kernels; however, we only report the results with a Gaussian kernel to save some space.

5.1 Performance Metric: Out of Sample R^2

We employ out-of-sample R^2 relative to the historical mean as our performance metric to assess various forecasting methods alongside our own. Out-of-sample R^2 indicates goodness of fit on unseen data, providing insights into the predictive accuracy of a model. Mathematically, out-of-sample R^2 is computed as follows:

$$R^2 = 1 - \frac{\sum_{i \in \text{test-data}} (y_i - \hat{y}_i)^2}{\sum_{i \in \text{test-data}} (y_i - \bar{y}_{\text{train}})^2}$$

Here, the numerator quantifies the squared deviation between the model's predictions and the true values in the test data. At the same time, the denominator measures the deviation of the true values from the historical mean in the test data. It is important to note that we utilize the mean of the training data for the historical mean, as in real-world forecasting scenarios, access to the training mean is typically available.

It is noteworthy that out-of-sample R^2 ranges from $-\infty$ to 1, unlike in-sample R^2, which ranges from zero to one. A positive out-of-sample R^2 indicates that the forecasting method outperforms the historical average. At the same time, a negative value suggests that the forecasting method performs worse than a simple method that forecasts y_i equal to the historical average.

We adopt the rolling window method to compute out-of-sample R^2, consistent with standard practices in the literature. Appendix B.1 provides a detailed exposition of our methodology.

5.2 Data and Hyper-Parameter Tuning

We utilize the quarterly macroeconomic dataset, FRED-QD. It covers the time span of 1959-2023. This dataset encompasses a comprehensive array of variables exceeding 250, including macroeconomic (such as GDP, Consumption, and Investment), financial, labor market, housing, and industrial and manufacturing variables. Our forecasting endeavors focus on a single target time series while leveraging the remaining variables within the predictor set. Our main text shows the forecasting of important variables from various domains, such as macro, labor, housing, finance, prices, etc. For ease of reference, we present a tabulation comprising the mnemonic codes and details of the variables in the FRED-QD dataset alongside their counterparts in the Stock-Watson dataset in Appendix B.2.

5.2.1 Data Transformation

PCA encounters challenges when applied to nonstationary time series commonly found in economics and finance. Nonstationary variables lack a defined population mean, and the sample standard deviation tends to diverge as the number of observations increases. Onatski & Wang (2021) discusses some of the significant issues arising from applying PCA to nonstationary data in detail. Generally, researchers address this by manually examining each series to identify necessary transformations before computing principal components. Hamilton & Xi (2024) offers an improved method of transformation to achieve the stationarity of the predictor set. We use their method to remove nonstationarity from our data.

Scholars in the literature often employ sample periods devoid of structural breaks; for instance, Fan *et al.* (2023) says "There exist significant structural breaks for many variables around the year of financial crisis in 2008 which makes our data non-stationary even after performing the suggested transformations". Therefore, our study focuses on the stationary period spanning from 1965 to 2007[8]. For the sanity check, we conduct analyses on different

[8] Another indirect advantage of the choice of this sample period is that it gives us the number of samples less than the number of predictors ($T < N$), hence a truly high-dimensional scenario to test our method in.

combinations of the sample periods, including the entire available sample period from 1959 to 2023, and find no qualitative discrepancies in our findings.

In our main analysis, the sample period from 1964:Q4 to 2007:Q1 comprises $T = 170$ observations (periods) and $N = 176$ variables (predictors). While the data is initially available for around 250 series, those with missing values are removed; this leaves us with a total of 176 series. We adopt the rolling window methodology for model training and hyper-parameter tuning, utilizing 70% of the total observations as the width of the rolling window. We observe qualitatively similar performance across varying window sizes (50%, 60% of total data). Subsequently, we evaluate the forecasting performance on out-of-sample data and present the results in the tables.

5.2.2 Hyper-parameter Tuning

Our methodology incorporates the kernel as a fundamental element of the estimation process. However, the kernel function includes a hyperparameter that necessitates optimization. Concurrently, a similar hyperparameter requires tuning in the context of a competitor method, namely kernel PCA. Thus, we employ an identical tuning procedure for both methodologies. We adopt a Gaussian kernel, which relies on a single hyperparameter, denoted as σ, for our specific applications. Due to the nature of our dataset, which comprises time series data, conventional methods such as random sampling for k-fold cross-validation are not directly applicable. Instead, we partition the data into two folds and conduct cross-validation to determine the optimal tuning parameter. Further elaboration on the algorithm employed for this purpose is provided in the appendix-B.3.

Furthermore, among our competitive methodologies, certain approaches are based on PCA, necessitating the judicious selection of the number of principal components to be included in the analysis. To address this, we employ the eigenvalue ratio test method proposed by Ahn & Horenstein (2013). This method computes the ratio of each eigenvalue to its predecessor and selects the number of principal components corresponding to the index where this ratio attains its maximum value.

5.3 Forecasting Using Theory Guided Proxies

We show the utility of theory-guided proxies as in Kelly & Pruitt (2015) to predict certain variables. In this section, we present a comparison with the linear benchmark, i.e., 3PRF.

The primary strength of our methodology lies in its ability to accurately forecast over longer horizons, where non-linear relationships become more pronounced. However, for the purposes of this section, we restrict our analysis to one-period ahead forecasting. Our results show that our approach outperforms its closest competitor even in the short term. It is essential to note that the primary objective of this subsection is to establish the viability of theory-guided proxies rather than to conduct a comprehensive comparison with competing methods. A more extensive performance evaluation will be presented in subsequent subsections, where we used the auto-proxy method discussed in table-3 to construct forecasts using Kernel 3PRF.

5.3.1 National Income Identity

Sometimes, the context of the problem gives us good choices for proxy variables. There is ample evidence that consumption and investments can be reasonable proxies for a country's gross domestic product (GDP). The two proxies affect the GDP through the multiplier effect. Therefore, for the GDP (Y), we can choose consumption (C) and Investment (I) as proxy variables. We forecast GDP by taking combinations of consumption and investment as proxies. The results are presented in Table-4.

Table 4: One-period Ahead Out-of-Sample R^2 for National Income

Proxy	3PRF	k3PRF
Consumption and Investment	0.621	0.768
Investment	0.627	0.748
Consumption	0.589	0.760

It is clear that using the proxies works, and our method performs better than the nearest competitive method Kelly & Pruitt (2015).

5.3.2 Quantity Theory of Money

In another application of theory-guided proxies, we utilize the quantity theory of money to forecast inflation using GDP and money supply as proxies. The quantity theory of money equation states:

$$\frac{\Delta(\text{Money supply}) \times \Delta(\text{Velocity of money})}{\Delta(\text{Real Product})} = \Delta(\text{Price level})$$

Our objective is to forecast inflation. In our dataset, Δ(Real Product) represents the change in GDP, while Δ(Money Supply) signifies the changes in money supply using log growth in M1. Similar to Fama (1981), changes in velocity, which are challenging to quantify, serve as the error term in the forecasting relationship. The timing is aligned such that proxies observed at time t are utilized to extract information from the predictors at time t for forecasting inflation at time $t+1$. The results for one-period ahead inflation forecasts are presented in Table-5.

Table 5: One-period Ahead Out-of-Sample R^2 for Inflation

Proxy	3PRF	k3PRF
GDP and Money Supply	0.265	0.265
GDP	0.037	0.037
Money Supply	0.350	0.355

The results indicate that the theory-guided proxies effectively capture inflation dynamics, yielding performance comparable to the closest competitor. It is important to emphasize again that this analysis focuses on one-step-ahead forecasts, which are not the primary strength of our methodology. The purpose of presenting these results is solely to demonstrate the efficacy of the proxies.

5.4 Long and Short-Run Forecasting: Comparative Performance Plots

Linear equations may approximate the relationships between targets and predictors effectively when the analysis time span is sufficiently short. However, as the time span expands, incorporating non-linearities becomes crucial, as noted by Goulet Coulombe *et al.* (2022). Linear methods exhibit deteriorating performance as the forecasting horizon extends into the future. Thus, the primary strength of our methodology lies in addressing longer-horizon forecasting challenges. Nevertheless, we demonstrate that even in shorter-horizon forecasting scenarios, our approach distinctly outperforms the nearest competitor Kelly & Pruitt (2015). In the subsequent section, we present comparative plots, reserving detailed and comprehensive comparisons for subsequent sub-sections.

5.4.1 Short Horizon Forecasting

While kernel functions are recognized for their ability to effectively capture non-linear relationships between variables, it's essential to acknowledge that linear relationships can also be effectively modeled by kernel functions by selecting an appropriate tuning hyperparameter.

In this sub-section, we aim to demonstrate the superiority of our kernel-based forecasting method over the closest linear forecasting method (3PRF) in the one-step-ahead forecasting problem. We present the one-step-ahead forecasted series using our method (k3PRF) and 3PRF alongside the true values of the target variables in figure-3. Specifically, we compare the performance across four different types of economic series from different domains: macro series Exports, price series GDP Deflator, manufacturing series Industrial Production, and financial series the S&P 500 Index.

The plots in figure-3 clearly illustrate that our predictions closely align with the true series, surpassing the predictions generated by 3PRF. Our method captures significant fluctuations, including notable drops and peaks, demonstrating its efficacy in short-term forecasting scenarios.

5.4.2 Long Horizon Forecasting

In this section, we plot the long-horizon (twelve periods ahead) forecasts generated by the 3PRF method and our method against the actual value of the target series in figure-4. We compare the two methods on the same four economic series as in the previous subsection.

Figure 3: Short Horizon (One period ahead) Forecasting: Comparative Performance

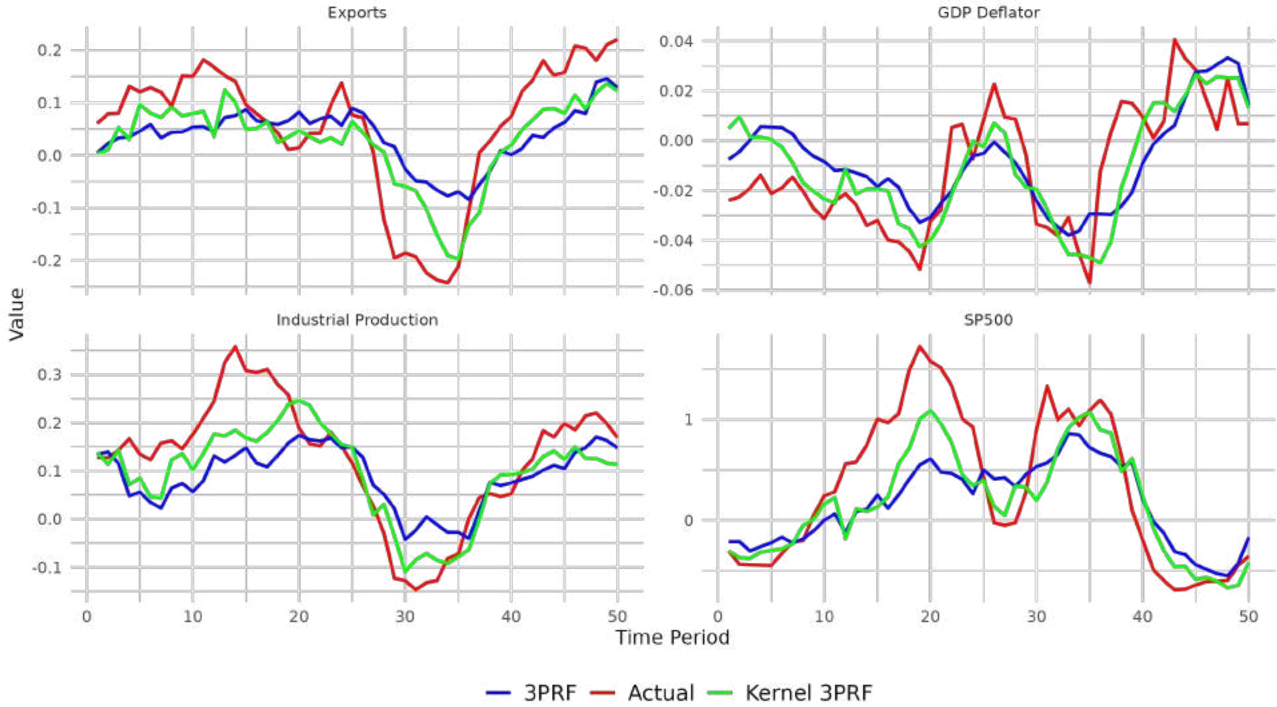

We observe that the long-horizon forecasts of our competitor, the 3PRF method, tend to flatter, i.e., approaching a historical mean. Whereas our method can accurately track the true series by capturing ups and downs. Although it is acknowledged that absolute predictability may diminish over longer horizons relative to linear methods, our approach continues to demonstrate robust performance, even on extended forecasting horizons.

5.5 Forecasting Macroeconomic Variables

An astute economic decision, such as monetary policy formulation, hinges upon well-informed anticipations of future trends in macroeconomic and financial data. Consequently, forecasting macroeconomic variables emerges as a pivotal pursuit for economists. Quoting Federal Reserve of New York's website, Kim & Swanson (2014) notes, "In formulating the nation's monetary

Figure 4: Long Horizon (Twelve periods ahead) Forecasting: Comparative Performance

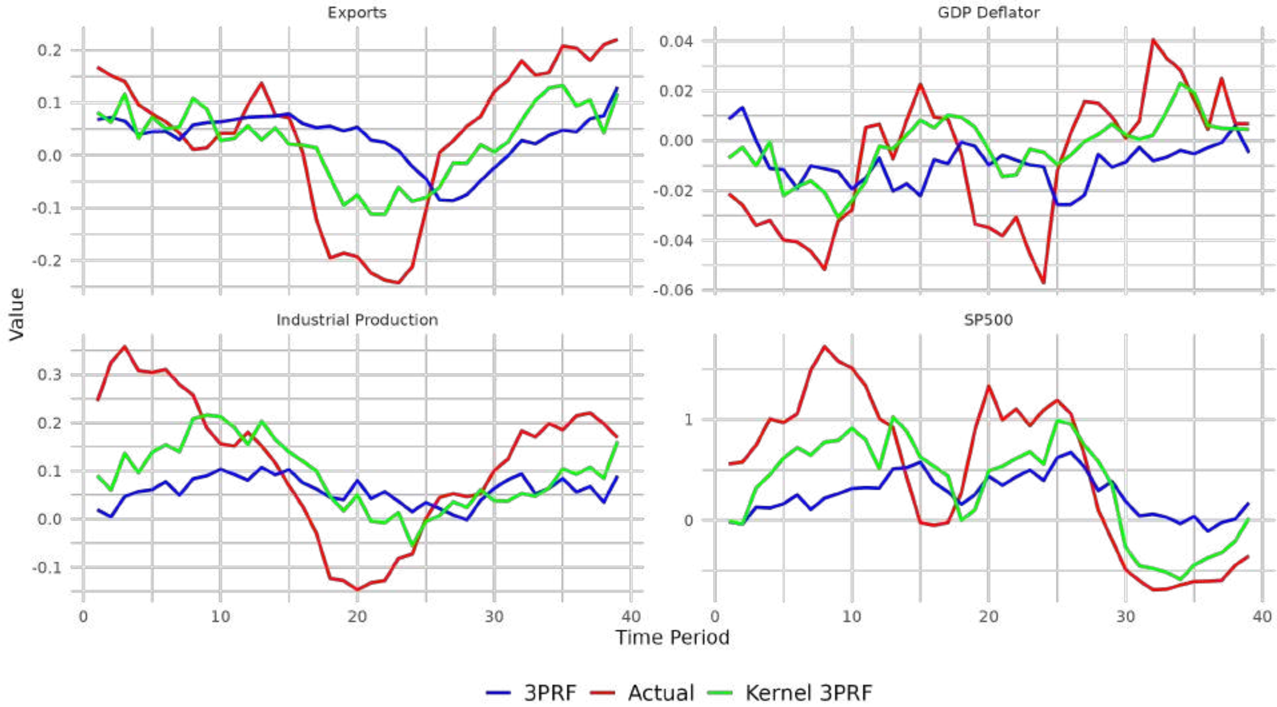

policy, the Federal Reserve considers a number of factors, including the economic and financial indicators which follow, as well as the anecdotal reports compiled in the Beige Book. Real Gross Domestic Product (GDP); Consumer Price Index (CPI); Nonfarm Payroll Employment Housing Starts; Industrial Production/Capacity Utilization; Retail Sales; Business Sales and Inventories; Advance Durable Goods Shipments, New Orders and Unfilled Orders; Lightweight Vehicle Sales; Yield on 10-year Treasury Bond; S&P 500 Stock Index; M2". We, therefore, aim to forecast some of these crucial indicators in this paper. We compare the performance of our model against the competitors. This section forecasts seven macro series: GDP, Consumption, Investment, Exports, Imports, Fixed Investment, and Industrial Production (Final).

Results and Disucssion To present the results in a tidy manner, we make two tables. In table-6, we present the forecasting performance on three series: GDP, Consumption, and In-

	Method	h=1	h=2	h=3	h=4	h=6	h=8	h=10	h=12
GDP									
	AR(2)	0.929	0.906	0.843	0.719	0.302	-0.216	-0.555	-0.724
	PCA	0.717	0.650	0.575	0.492	0.311	0.130	-0.001	-0.075
	Sq-PC	0.615	0.593	0.552	0.488	0.290	0.076	-0.092	-0.166
	PC-Sq	0.773	0.733	0.676	0.594	0.398	0.175	0.008	-0.063
	kPCA	0.638	0.589	0.528	0.464	0.322	0.204	0.060	0.063
	3PRF	0.667	0.619	0.561	0.493	0.341	0.193	0.130	0.201
	k3PRF	0.808	0.788	0.757	0.701	0.603	0.544	0.608	0.434
Consumption									
	Method	h=1	h=2	h=3	h=4	h=6	h=8	h=10	h=12
	AR(2)	0.957	0.943	0.892	0.805	0.485	0.015	-0.375	-0.557
	PCA	0.573	0.554	0.504	0.430	0.238	0.038	-0.093	-0.155
	Sq-PC	0.546	0.541	0.499	0.428	0.235	0.025	-0.137	-0.206
	PC-Sq	0.611	0.637	0.628	0.596	0.412	0.161	-0.041	-0.128
	kPCA	0.433	0.419	0.369	0.319	0.143	0.076	0.039	0.181
	3PRF	0.589	0.547	0.501	0.464	0.386	0.196	0.169	0.326
	k3PRF	0.713	0.730	0.720	0.741	0.770	0.747	0.275	0.496
Investment									
	Method	h=1	h=2	h=3	h=4	h=6	h=8	h=10	h=12
	AR(2)	0.830	0.807	0.711	0.546	0.087	-0.450	-0.544	-0.586
	PCA	0.516	0.393	0.300	0.231	0.149	0.089	0.030	0.011
	Sq-PC	0.398	0.348	0.297	0.238	0.099	-0.022	-0.083	-0.065
	PC-Sq	0.605	0.488	0.391	0.296	0.186	0.090	0.017	0.044
	kPCA	0.479	0.390	0.317	0.272	0.196	0.030	-0.016	-0.013
	3PRF	0.597	0.484	0.429	0.369	0.273	0.111	0.083	0.176
	k3PRF	0.760	0.640	0.478	0.605	0.433	0.199	0.169	0.389

Table 6: h-period ahead out of sample R^2 of Macro Variables : Group-I

vestment. To keep track of the presentation, we informally call it 'Group-I'. Table-7 shows comparative forecasting performance on 'Group-II' macro variables: Exports, Imports, Fixed Investments, and Industrial Production (Final Index). Further detail on these variable series is available in appendix-B.2. The numbers reported in the table are out of sample R^2 defined earlier in the text. We present performance for various forecast horizons ranging from one period ahead to twelve periods ahead.

An empirical observation highlights that among various unsupervised forecasting methodolo-

	Method	h=1	h=2	h=3	h=4	h=6	h=8	h=10	h=12
Exports									
	AR(2)	0.928	0.926	0.906	0.863	0.723	0.522	0.409	0.302
	PCA	0.353	0.306	0.248	0.193	0.123	0.107	0.106	0.109
	Sq-PC	0.275	0.249	0.215	0.183	0.120	0.056	0.008	-0.013
	PC-Sq	0.399	0.326	0.243	0.166	0.073	0.066	0.113	0.194
	kPCA	0.027	0.033	0.033	0.270	0.142	-0.002	-0.044	0.130
	3PRF	0.535	0.523	0.459	0.389	0.223	0.137	0.109	0.092
	k3PRF	0.724	0.705	0.641	0.602	0.546	0.575	0.600	0.631
Imports	Method	h=1	h=2	h=3	h=4	h=6	h=8	h=10	h=12
	AR(2)	0.969	0.964	0.951	0.931	0.845	0.710	0.577	0.460
	PCA	0.417	0.380	0.343	0.306	0.233	0.154	0.072	0.006
	Sq-PC	0.395	0.373	0.341	0.299	0.194	0.079	-0.005	-0.046
	PC-Sq	0.477	0.462	0.438	0.398	0.306	0.182	0.060	0.000
	kPCA	0.421	0.389	0.348	0.311	0.241	0.081	0.064	0.033
	3PRF	0.546	0.506	0.468	0.436	0.394	0.347	0.322	0.338
	k3PRF	0.777	0.783	0.790	0.786	0.749	0.411	0.388	0.558
Fixed Invest.	Method	h=1	h=2	h=3	h=4	h=6	h=8	h=10	h=12
	AR(2)	0.905	0.881	0.818	0.682	0.224	-0.267	-0.467	-0.605
	PCA	0.490	0.384	0.290	0.220	0.134	0.088	0.042	0.016
	Sq-PC	0.401	0.352	0.293	0.231	0.095	-0.024	-0.077	-0.064
	PC-Sq	0.595	0.492	0.385	0.314	0.208	0.104	0.030	0.068
	kPCA	0.498	0.407	0.315	0.250	0.167	0.039	-0.034	0.007
	3PRF	0.525	0.454	0.389	0.348	0.251	0.122	0.127	0.226
	k3PRF	0.736	0.659	0.426	0.578	0.265	0.235	0.261	0.359
IP : Final	Method	h=1	h=2	h=3	h=4	h=6	h=8	h=10	h=12
	AR(2)	0.830	0.807	0.711	0.546	0.087	-0.450	-0.544	-0.586
	PCA	0.516	0.393	0.300	0.231	0.149	0.089	0.030	0.011
	Sq-PC	0.398	0.348	0.297	0.238	0.099	-0.022	-0.083	-0.065
	PC-Sq	0.605	0.488	0.391	0.296	0.186	0.090	0.017	0.044
	kPCA	0.479	0.390	0.317	0.272	0.196	0.030	-0.016	-0.013
	3PRF	0.597	0.484	0.429	0.369	0.273	0.111	0.083	0.176
	k3PRF	0.760	0.640	0.478	0.605	0.433	0.199	0.169	0.389

Table 7: h-period ahead out of sample R^2 of Macro Variables : Group-II

gies, including PCA, Squared-PC, PC-squared, and non-linear unsupervised approaches such as kernel PCA, none exhibit superior performance compared to our proposed method across any forecast horizon for the seven series under consideration. While the supervised linear forecasting model 3PRF demonstrates improved performance relative to the unsupervised techniques, it still falls short of outperforming our non-linear supervised approach. Notably, the autoregressive (AR) model emerges as the sole contender capable of surpassing our method in the short term. Remarkably, our approach exhibits only a marginal performance differential compared to the AR model in shorter forecast horizons yet significantly outperforms it over longer forecast horizons.

In summary, the consistent empirical observation across all series suggests that our method progressively outperforms all alternative methodologies with increasing forecast horizons. Notably, the AR model remains a competitive rival in the short term, attributed to the linear model's relative advantage in capturing short-term dynamics where nonlinearities may not yet manifest. Consequently, our method emerges as a dependable and preferred forecasting framework across all forecast horizons in macroeconomic prediction tasks.

5.6 Forecasting Labor Market Variables

The examination of the unemployment rate and total non-farm employment offers a deeper understanding of the labor market dynamics within an economy. The labor market is a pivotal element given its centrality in providing income and livelihoods for most economic actors. Consequently, fluctuations in the labor market exert profound impacts on consumer spending patterns and inflationary pressures. These indicators serve as crucial inputs into important economic decisions, notably informing the formulation of both fiscal and monetary policies to achieve goals. We forecast these two series and present the results in table-8.

Result and Discussions We present the results in table-8. It's worth noting that the overall trends in the total non-farm employment series align with our macroeconomic time

Employment								
Method	h=1	h=2	h=3	h=4	h=6	h=8	h=10	h=12
AR(2)	0.992	0.961	0.864	0.693	0.170	-0.429	-0.881	-1.079
PCA	0.786	0.728	0.604	0.435	0.057	-0.219	-0.258	-0.146
Sq-PC	0.528	0.498	0.440	0.361	0.167	-0.024	-0.109	-0.098
PC-Sq	0.836	0.795	0.679	0.510	0.131	-0.139	-0.210	-0.110
kPCA	0.832	0.790	0.702	0.587	0.370	0.196	0.112	0.059
3PRF	0.765	0.731	0.712	0.662	0.407	0.312	0.264	0.229
k3PRF	0.929	0.895	0.846	0.768	0.556	0.444	0.441	0.584
Unemp Rate								
Method	h=1	h=2	h=3	h=4	h=6	h=8	h=10	h=12
AR(2)	0.963	0.927	0.847	0.721	0.378	0.011	-0.150	-0.196
PCA	0.810	0.853	0.849	0.809	0.648	0.426	0.255	0.133
Sq-PC	0.825	0.852	0.849	0.821	0.686	0.457	0.251	0.097
PC-Sq	0.798	0.849	0.851	0.820	0.687	0.497	0.304	0.225
kPCA	0.610	0.664	0.672	0.675	0.647	0.562	0.440	-0.035
3PRF	0.913	0.914	0.863	0.802	0.638	0.475	0.402	0.471
k3PRF	0.924	0.937	0.903	0.846	0.674	0.508	0.459	0.390

Table 8: Out of Sample R^2 of Employment (non-farm) and Unemployment Rate

series discussion. Importantly, our method consistently outperforms competitors in longer horizon forecasting ($h \geq 4$), a testament to its robustness and reliability. As we extend the forecast horizons, the margin of our method's superior performance continues to grow, instilling confidence in its effectiveness. In the short term, our method may not outperform the autoregressive model, but it still ranks second and is only slightly behind. Similarly, in forecasting the unemployment rate, our method consistently outperforms all other methods, including the autoregressive (AR) model, from $h = 2$ onwards.

To summarize, our findings mirror those of the macroeconomic series forecasting. Our method consistently demonstrates superior performance across various forecast horizons and labor market indicators, reaffirming its reliability and preference in macroeconomic prediction tasks.

5.7 Forecasting Housing Variables

The housing market is characterized by its multidimensional aspect, involving various natures and functions. Houses serve as places of residence and vehicles for wealth accumulation, asset transfer to the next generation, and investment. Also, housing comprises a significant portion of household assets, making it an important factor in household decision-making. Consequently, distortions in the housing market can affect household spending and the broader economy through institutions such as mortgage banks. Therefore, forecasting housing market activities holds substantial value. In this section, we forecast two housing series: the first is Privately Owned Housing Starts (*HStart*), and the second is Privately Owned Housing Starts in the Western Census region(*HStart-W*).

Table 9: Out of Sample R^2 of Privately Owned Housing Starts: Total and West Region

HStart

Method	h=1	h=2	h=3	h=4	h=6	h=8	h=10	h=12
AR(2)	0.048	-0.029	-0.140	-0.216	-0.380	-0.157	-0.131	-0.105
PCA	-1.360	-0.799	-0.317	-0.052	0.172	0.259	0.086	0.085
Sq-PC	-1.226	-0.688	-0.196	0.095	0.314	0.453	0.183	0.100
PC-Sq	-1.473	-0.936	-0.371	-0.004	0.278	0.188	-0.176	-0.024
kPCA	-0.199	-0.074	-0.157	0.244	0.408	-0.101	-0.325	0.101
3PRF	0.092	0.272	0.064	-0.223	-0.391	-0.205	-0.220	-0.653
k3PRF	0.138	0.204	0.231	0.245	0.230	0.253	0.116	0.073

HStart-W

Method	h=1	h=2	h=3	h=4	h=6	h=8	h=10	h=12
AR(2)	0.571	0.540	0.495	0.386	0.003	-0.397	-0.402	-0.787
PCA	0.326	0.433	0.481	0.516	0.405	0.169	-0.070	-0.182
Sq-PC	0.201	0.318	0.356	0.372	0.184	-0.053	-0.248	-0.323
PC-Sq	0.359	0.402	0.414	0.459	0.310	0.033	-0.135	-0.244
kPCA	0.287	0.336	0.379	0.442	0.447	-0.135	-0.147	-0.062
3PRF	0.571	0.475	0.231	0.084	-0.031	0.094	0.260	0.253
k3PRF	0.586	0.464	0.207	0.554	0.178	0.141	0.160	0.463

Results and Discussions– Table-9 presents the forecasting results. One can note that predicting the privately owned housing start time series is very difficult. While most forecasting methods cannot beat the historical average, our method performs better than all other methods at all horizons. On the other hand, while it is relatively easy to forecast housing in the western census region, our method performs better than all other methods except for one or two cases. The results in other housing variables follow similar patterns; therefore, we omit them for the simplicity of exposition.

Therefore, it is clear that our method holds value in a difficult forecasting problem in both the short and long run. We also enjoy a better method for long-run forecasting problems in the housing market series.

5.8 Forecasting Price Variables

Inflation, a topic of significant interest in the market, media, and academia, holds a crucial role due to its impact on the common consumers. Particularly, inflation adversely affects low-wage earners, underscoring its societal implications. The relevance of our research is underscored by the fact that one of the primary objectives of the Federal Reserve or Central Bank is to control inflation. In this context, we focus on forecasting two key price time series: the GDP Deflator and the Consumer Price Index (CPI), which are pivotal in understanding and predicting inflation. The motivation behind choosing these two price series is that– on the one hand, the GDP Deflator considers the macroeconomic picture at the aggregate level. At the same time, the CPI measure informs us of the inflation faced by the consumer at a disaggregated level.

Results and Discussion Table-10 presents the results. It reiterates almost the same story we discussed in previous subsections. In both series, we dominate all other methods at all forecast horizons. While we marginally lag the AR model at some short horizons, we decisively beat it in longer horizons.

GDP Deflator

Method	h=1	h=2	h=3	h=4	h=6	h=8	h=10	h=12
AR(2)	0.797	0.774	0.740	0.657	0.418	0.146	0.156	0.077
PCA	0.444	0.276	0.056	-0.184	-0.408	-0.347	-0.221	-0.057
Sq-PC	0.299	0.145	-0.035	-0.168	-0.245	-0.230	-0.192	-0.108
PC-Sq	0.431	0.268	0.104	-0.039	-0.106	-0.038	-0.111	-0.182
kPCA	-0.032	0.247	-0.021	0.008	0.003	0.004	0.029	-0.023
3PRF	0.584	0.496	0.426	0.243	0.174	0.279	0.300	0.155
k3PRF	0.667	0.632	0.563	0.476	0.479	0.413	0.197	0.512

CPI

Method	h=1	h=2	h=3	h=4	h=6	h=8	h=10	h=12
AR(2)	0.704	0.706	0.620	0.565	0.397	0.211	0.062	-0.038
PCA	0.660	0.535	0.364	0.154	-0.163	-0.252	-0.248	-0.173
Sq-PC	0.410	0.296	0.161	0.049	-0.055	-0.156	-0.200	-0.173
PC-Sq	0.649	0.512	0.353	0.186	-0.019	-0.087	-0.187	-0.228
kPCA	0.440	0.380	-0.050	0.189	-0.043	-0.024	0.042	-0.006
3PRF	0.641	0.566	0.487	0.352	0.192	0.241	0.255	0.141
k3PRF	0.676	0.612	0.541	0.463	0.469	0.434	0.349	0.477

Table 10: Out of Sample R^2 of Price Variables (Chain-type Price Indices)

5.9 Forecasting Financial Variables

While the necessity for forecasting financial variables may seem self-evident, it is pertinent to underscore the significance of such endeavors. The collective market capitalization of companies constituting the S&P 500 stands at approximately 43 trillion US dollars, underscoring the substantial economic weight of these entities. While stock market indices, including the S&P 500, are typically considered risky financial assets, government securities represent their low-risk counterpart. Within this sub-section, we forecast both risky (S&P 500 Index), safe (GS-1), and one in-between (GS-10) financial series.

Results and Discussion There is nothing new regarding the patterns of the forecasting performance we are observing. The GS-1 means government securities (Treasury Bills), which mature in one year, and similarly, the GS-10 means the treasury notes, which mature in 10 years. Our method beats all other methods except the AR model on all forecast horizons for

GS-1

Method	h=1	h=2	h=3	h=4	h=6	h=8	h=10	h=12
AR(2)	0.915	0.862	0.796	0.645	0.184	-0.270	-0.304	-0.336
PCA	0.687	0.487	0.261	0.055	-0.163	-0.124	-0.033	0.139
Sq-PC	0.306	0.201	0.090	-0.012	-0.145	-0.131	-0.074	0.011
PC-Sq	0.674	0.448	0.243	0.059	-0.162	-0.119	0.051	0.163
kPCA	0.635	0.472	0.282	0.119	0.029	-0.018	0.166	0.114
3PRF	0.856	0.735	0.615	0.501	0.449	0.329	0.241	0.349
k3PRF	0.873	0.806	0.782	0.699	0.381	0.224	0.428	0.605

GS-10

Method	h=1	h=2	h=3	h=4	h=6	h=8	h=10	h=12
AR(2)	0.783	0.766	0.667	0.540	0.237	-0.022	0.057	0.136
PCA	0.446	0.327	0.148	0.017	-0.122	-0.177	-0.329	-0.378
Sq-PC	0.312	0.247	0.124	0.069	-0.016	-0.065	-0.194	-0.327
PC-Sq	0.421	0.292	0.200	0.155	0.117	0.032	-0.083	-0.608
kPCA	0.457	0.402	-0.098	0.246	-0.039	-0.022	0.082	0.035
3PRF	0.615	0.469	0.268	0.012	0.168	0.403	0.294	0.044
k3PRF	0.621	0.499	0.405	0.401	0.345	0.272	0.161	0.566

S&P 500

Method	h=1	h=2	h=3	h=4	h=6	h=8	h=10	h=12
AR(2)	0.953	0.943	0.912	0.866	0.697	0.456	0.277	0.272
PCA	0.388	0.318	0.224	0.121	-0.019	-0.001	0.107	0.201
Sq-PC	0.265	0.214	0.152	0.089	0.023	0.061	0.136	0.192
PC-Sq	0.387	0.287	0.167	0.048	-0.079	0.034	0.220	0.295
kPCA	-0.064	-0.067	-0.039	-0.031	0.094	0.038	0.091	0.558
3PRF	0.706	0.687	0.636	0.566	0.453	0.458	0.489	0.523
k3PRF	0.812	0.791	0.736	0.654	0.565	0.586	0.674	0.781

Table 11: Out of Sample R^2 of Financial Market Series

all the series discussed here. While marginally lag the AR model in the short run, we beat it decisively in the longer horizon forecasts.

6 Comparing the Performance on All Series

To enhance the robustness of our empirical analysis, we conducted comparative assessments of our method against competing methods across all 176 series within our dataset. This entailed selecting each series as the target and repeating the comparative analysis for every series in our dataset. This subsection reports comprehensive competitive assessments of forecasting that are under consideration against our method.

6.1 Description of Comparisons

We conducted the forecast comparisons across eight horizons, denoted as $h = 1, 2, 3, 4, 6, 8, 10, 12$. Consequently, our investigation encompasses the comparative performance of models across a total of $176 \times 8 = 1408$ combinations. The results of these comparisons, indicating the percentage of instances where a particular method demonstrated superior performance, are presented in Table 17. For example, if a method emerged as the best performer in 704 out of 1408 combinations, it would be represented by a value of 50 in the table. In simpler words, we count the relative frequency of the occurrence of the best performance of a given method and express it in percentage terms.

While the preceding frequency comparisons provide insight into the number of times each method proved superior to others, they do not measure the extent to which the best-performing method surpassed its nearest competitor. In other words, while method A may marginally outperform method B on one forecast horizon, method B might exhibit a considerable advantage over method A on another horizon, and then the aforementioned frequency comparison may not present the full picture. To account for this measure, we introduce a notion of '*Tolerance*' level. We call a method 'best' under tolerance level ϵ if the out-of-sample R^2 of a method is within ϵ percentage lower than the best method's performance. For example, suppose the AR model is the best for a combination of series y and $h = h_0$ with a $R^2 = 0.60$. For tolerance=5, another method will also be considered 'best' if its R^2 is greater than or equal to

$0.60(1 - 5/100) = 0.57$. Therefore, for a non-zero tolerance, it is possible to have multiple 'best' methods. When we set tolerance=0, the method counts relative frequencies.

The "Overall" set of rows presents the percentage of instances where a method outperformed all other methods or lies in the tolerance range of the best-performing method among all 1408 comparisons. Recognizing that forecast objectives may vary in time horizon, we scrutinize comparative performances in short- and long-run contexts. The "Short-run" rows incorporate horizons $h = 1, 2, 3, 4$, comprising 708 (calculated as 176×4) combinations, while the "Long-run" row includes horizons $h = 6, 8, 10, 12$, similarly amounting to 708 combinations. Additionally, we present a row labeled "Without AR", wherein we exclude the auto-regressive method and compare the remaining methodologies. Going beyond short and long-run analysis, we enrich our analysis by reporting similar comparative performance numbers for each forecast horizon h. These numbers are reported in the appendix-B.5.

Before closing this section, we want to clarify that since multiple 'best' methods are possible for a non-zero tolerance level, the sum of rows can exceed 100 percent for non-zero tolerance. For tolerance=0, the rows sum up to 100 percent.

6.2 Results

We present the results into table-12. The findings presented in this study yield several noteworthy observations. First, it is evident that unsupervised forecasting techniques, including PCA, Squared-PC, PC-squared, and kernel PCA, exhibit inferior performance across the majority of scenarios when compared to our method. Second, our method, kernel 3PRF, demonstrates unequivocal superiority in long-term forecasting endeavors. Third, our method is unequivocally superior in the absence of the AR method. Our method does not outperform AR in the short term, but its performance remains competitive, often closely trailing the best short-run autoregressive method. This can be seen by increasing the tolerance level. We can see that the instances where our method can be labeled as 'best' increase rapidly as we increase the tolerance level.

Analysis	Tolerance(%)	Methods						
		AR(2)	**PCA**	**Sq-PC**	**PC-Sq**	**kPCA**	**3PRF**	**k3PRF**
Overall								
	0	48.22	0.21	0.85	1.42	2.98	6.47	39.56
	5	50.07	1.14	1.35	1.99	3.34	9.16	43.54
	10	52.41	2.27	2.13	3.34	4.26	13.07	48.37
	20	55.68	5.68	3.69	7.74	6.75	23.30	62.57
Short-run								
	0	84.09	0.14	0.43	0.57	0.43	1.70	12.64
	5	87.07	1.42	0.71	1.56	0.57	5.11	18.75
	10	90.77	3.27	1.70	3.84	1.28	9.23	26.14
	20	94.32	8.38	3.41	10.37	3.55	20.03	48.72
Long-run								
	0	12.36	0.28	1.28	2.27	5.54	11.79	66.48
	5	13.07	0.85	1.99	2.41	6.11	13.21	68.32
	10	14.06	1.28	2.56	2.84	7.24	16.90	70.60
	20	17.05	2.98	3.98	5.11	9.94	26.56	76.42
Without AR								
	0	-	1.42	1.56	2.84	5.47	13.00	75.71
	5	-	2.84	2.06	4.76	5.75	17.97	78.76
	10	-	5.26	3.27	7.74	7.03	25.99	81.53
	20	-	11.08	5.89	14.35	11.43	41.34	86.08

Table 12: Distribution of Best Forecasting Methods Across All Series in Our Data (Percentage)

In summary, the table offers insights into the overall efficacy of our method across various forecast horizons. While the autoregressive (AR) method may exhibit marginal superiority in short-term forecasts, this advantage is notably slim. Conversely, when our method surpasses AR, it does so considerably. Consequently, our method emerges as a dependable and preferred choice for forecasting across all horizons, offering robust and consistent performance.

7 Conclusion

Building upon the three-pass regression filter by Kelly & Pruitt (2015), we introduce a new forecasting method, kernel three-pass regression filter. Our contention is that this approach holds promise as a dependable forecasting tool in environments characterized by approximate latent factor structure in predictors owing to two primary factors.

Firstly, it adeptly integrates non-linear relationships by transforming input data into a higher-dimensional space encapsulating its non-linear functions. Secondly, it operates as a supervised method, effectively filtering out and discarding useless factors to predict the target variable. We prove that the forecast generated by our method converges to the best infeasible forecast in probability as both N and T grow large.

We compare our method with competitor methods on 176 times series in FRED-QD data. Our findings consistently indicate that our methodology outperforms all competitors, particularly in longer-term forecasting scenarios across most time series under examination. The autoregressive (AR) method is the sole contender in short-term forecasting challenges. While the AR method may exhibit a marginal edge in short-term predictions, the differential advantage is negligible. Conversely, in instances where our methodology surpasses the AR method, it does so significantly. Consequently, our approach is dependable and preferred for forecasting across all temporal horizons, ensuring robust and steadfast performance.

References

Ahn, Seung C, & Horenstein, Alex R. 2013. Eigenvalue ratio test for the number of factors. *Econometrica*, **81**(3), 1203–1227.

Bai, Jushan. 2003. Inferential theory for factor models of large dimensions. *Econometrica*, **71**(1), 135–171.

Bai, Jushan, & Ng, Serena. 2006. Confidence intervals for diffusion index forecasts and inference for factor-augmented regressions. *Econometrica*, **74**(4), 1133–1150.

Bai, Jushan, & Ng, Serena. 2008. Forecasting economic time series using targeted predictors. *Journal of Econometrics*, **146**(2), 304–317.

Chamberlain, Gary, & Rothschild, Michael. 1983. Arbitrage, Factor Structure, and Mean-

Variance Analysis on Large Asset Markets. *Econometrica: Journal of the Econometric Society*, 1281–1304.

Cook, R Dennis. 2018. Principal components, sufficient dimension reduction, and envelopes. *Annual Review of Statistics and Its Application*, **5**, 533–559.

Exterkate, Peter, Groenen, Patrick JF, Heij, Christiaan, & van Dijk, Dick. 2016. Nonlinear forecasting with many predictors using kernel ridge regression. *International Journal of Forecasting*, **32**(3), 736–753.

Fan, Jianqing, Xue, Lingzhou, & Yao, Jiawei. 2017. Sufficient forecasting using factor models. *Journal of econometrics*, **201**(2), 292–306.

Fan, Jianqing, Lou, Zhipeng, & Yu, Mengxin. 2023. Are latent factor regression and sparse regression adequate? *Journal of the American Statistical Association*, 1–13.

Goulet Coulombe, Philippe, Leroux, Maxime, Stevanovic, Dalibor, & Surprenant, Stéphane. 2022. How is machine learning useful for macroeconomic forecasting? *Journal of Applied Econometrics*, **37**(5), 920–964.

Hamilton, James D, & Xi, Jin. 2024. *Principal Component Analysis for Nonstationary Series.* Tech. rept. National Bureau of Economic Research.

Huang, Dashan, Jiang, Fuwei, Li, Kunpeng, Tong, Guoshi, & Zhou, Guofu. 2022. Scaled PCA: A new approach to dimension reduction. *Management Science*, **68**(3), 1678–1695.

Kelly, Bryan, & Pruitt, Seth. 2015. The three-pass regression filter: A new approach to forecasting using many predictors. *Journal of Econometrics*, **186**(2), 294–316.

Kim, Hyun Hak, & Swanson, Norman R. 2014. Forecasting financial and macroeconomic variables using data reduction methods: New empirical evidence. *Journal of Econometrics*, **178**, 352–367.

Kutateladze, Varlam. 2022. The kernel trick for nonlinear factor modeling. *International Journal of Forecasting*, **38**(1), 165–177.

Li, Bing. 2018. *Sufficient dimension reduction: Methods and applications with R*. Chapman and Hall/CRC.

Onatski, Alexei, & Wang, Chen. 2021. Spurious factor analysis. *Econometrica*, **89**(2), 591–614.

Stock, James H, & Watson, Mark W. 2002a. Forecasting using principal components from a large number of predictors. *Journal of the American statistical association*, **97**(460), 1167–1179.

Stock, James H, & Watson, Mark W. 2002b. Macroeconomic forecasting using diffusion indexes. *Journal of Business & Economic Statistics*, **20**(2), 147–162.

A Technical Appendix

A.1 Proofs of Theoretical Results

Lemma 1 *Under Assumption(s) 1-3, we have the following*

1. $T^{-1/2}\boldsymbol{F}'\boldsymbol{J}_T\boldsymbol{\omega} = \boldsymbol{O}_p(1)$
2. $T^{-1/2}\boldsymbol{F}'\boldsymbol{J}_T\boldsymbol{\eta} = \boldsymbol{O}_p(1)$
3. $T^{-1/2}\boldsymbol{\varepsilon}'\boldsymbol{J}_T\boldsymbol{\eta} = \boldsymbol{O}_p(1)$
4. $M^{-1/2}\varepsilon_t'\boldsymbol{\Phi} = \boldsymbol{O}_p(1)$
5. $M^{-1}T^{-1}\boldsymbol{\Phi}'\boldsymbol{\varepsilon}'\boldsymbol{J}_T\boldsymbol{F} = \boldsymbol{O}_p\left(\delta_{MT}^{-1}\right)$
6. $M^{-1}T^{-1/2}\boldsymbol{\Phi}'\boldsymbol{\varepsilon}'\boldsymbol{J}_T\boldsymbol{\omega} = \boldsymbol{O}_p\left(1\right)$
7. $M^{-1/2}T^{-1/2}\boldsymbol{\Phi}\boldsymbol{\varepsilon}'\boldsymbol{J}_T\boldsymbol{\eta} = \boldsymbol{O}_p(1)$

8. $M^{-1}T^{-3/2}\boldsymbol{F}'\boldsymbol{J}_T\boldsymbol{\varepsilon}\boldsymbol{\varepsilon}'\boldsymbol{J}_T\boldsymbol{F} = \boldsymbol{O}_p\left(\delta_{MT}^{-1}\right)$

9. $M^{-1}T^{-3/2}\boldsymbol{\omega}'\boldsymbol{J}_T\varepsilon\boldsymbol{\varepsilon}'\boldsymbol{J}_T\boldsymbol{F} = \boldsymbol{O}_p\left(\delta_{MT}^{-1}\right)$

10. $M^{-1}T^{-3/2}\boldsymbol{\omega}'\boldsymbol{J}_T\varepsilon\varepsilon'\boldsymbol{J}_T\boldsymbol{\omega} = \boldsymbol{O}_p\left(\delta_{MT}^{-1}\right)$

11. $M^{-1}T^{-1/2}\boldsymbol{F}'\boldsymbol{J}_T\varepsilon\boldsymbol{\varepsilon}_t = \boldsymbol{O}_p\left(\delta_{MT}^{-1}\right)$

12. $M^{-1}T^{-1/2}\boldsymbol{\omega}'\boldsymbol{J}_T\varepsilon\varepsilon_t = \boldsymbol{O}_p\left(\delta_{MT}^{-1}\right)$

13. $M^{-1}T^{-3/2}\boldsymbol{\eta}'\boldsymbol{J}_T\varepsilon\varepsilon'\boldsymbol{J}_T\boldsymbol{F} = \boldsymbol{O}_p\left(\delta_{MT}^{-1}\right)$

14. $M^{-1}T^{-3/2}\boldsymbol{\eta}'\boldsymbol{J}_T\varepsilon\varepsilon'\boldsymbol{J}_T\boldsymbol{F} = \boldsymbol{O}_p\left(\delta_{MT}^{-1}\right)$

15. $T^{-1/2}\sum_t \eta_{t+h} = O_p(1)$

Proof: Proof can be seen from Kelly & Pruitt (2015), Lemma 2 in their appendix. The only difference is the omission of the matrix $\boldsymbol{J}_N$ in the various expressions. This, however, doesn't affect the rates, as can be verified from their proofs. We do not allow an intercept in pass-2 because doing so will require demeaning of the transformed predictor(s), which is not feasible.

Lemma 2 *Under Assumption(s) 1-5, we have the following*

1. $M^{-1}T^{-1}\boldsymbol{Z}'\boldsymbol{J}_T\varphi(\boldsymbol{X})\varphi(\boldsymbol{x}_t) = \boldsymbol{\Lambda}\boldsymbol{\Delta}_F\mathcal{P}\boldsymbol{F}_t + \boldsymbol{O}_p\left(\delta_{MT}^{-1}\right)$

2. $M^{-1}T^{-2}\boldsymbol{Z}'\boldsymbol{J}_T\varphi(\boldsymbol{X})\varphi(\boldsymbol{X})'\boldsymbol{J}_T\boldsymbol{y} = \boldsymbol{\Lambda}\boldsymbol{\Delta}_F\mathcal{P}\boldsymbol{\Delta}_F\boldsymbol{\beta} + \boldsymbol{O}_p\left(\delta_{MT}^{-1}\right)$

3. $M^{-2}T^{-3}\boldsymbol{Z}'\boldsymbol{J}_T\varphi(\boldsymbol{X})\varphi(\boldsymbol{X})'\boldsymbol{J}_T\varphi(\boldsymbol{X})\varphi(\boldsymbol{X})'\boldsymbol{J}_T\boldsymbol{Z} = \boldsymbol{\Lambda}\boldsymbol{\Delta}_F\mathcal{P}\boldsymbol{\Delta}_F\mathcal{P}\boldsymbol{\Delta}_F\boldsymbol{\Lambda}' + \boldsymbol{O}_p\left(\delta_{MT}^{-1}\right)$

Proof: The Proof follows directly by writing out the expressions. Item 1

$$\begin{aligned}
M^{-1}T^{-1}\boldsymbol{Z}'\boldsymbol{J}_T\varphi(\boldsymbol{X})\varphi(\boldsymbol{x}_t) &= \boldsymbol{\Lambda}\left(T^{-1}\boldsymbol{F}'\boldsymbol{J}_T\boldsymbol{F}\right)\left(M^{-1}\boldsymbol{\Phi}'\boldsymbol{\Phi}\right)\boldsymbol{F}_t + \boldsymbol{\Lambda}\left(T^{-1}\boldsymbol{F}'\boldsymbol{J}_T\boldsymbol{F}\right)\left(M^{-1}\boldsymbol{\Phi}'\boldsymbol{\varepsilon}_t\right) \\
&+ \boldsymbol{\Lambda}\left(M^{-1}T^{-1}\boldsymbol{F}'\boldsymbol{J}_T\boldsymbol{\varepsilon}\boldsymbol{\Phi}\right)\boldsymbol{F}_t + \boldsymbol{\Lambda}\left(M^{-1}T^{-1}\boldsymbol{F}'\boldsymbol{J}_T\boldsymbol{\varepsilon}\boldsymbol{\varepsilon}_t\right) \\
&+ \left(T^{-1}\boldsymbol{\omega}'\boldsymbol{J}_T\boldsymbol{F}\right)\left(M^{-1}\boldsymbol{\Phi}'\boldsymbol{\Phi}\right)\boldsymbol{F}_t + \left(T^{-1}\boldsymbol{\omega}'\boldsymbol{J}_T\boldsymbol{F}\right)\left(M^{-1}\boldsymbol{\Phi}'\boldsymbol{\varepsilon}_t\right) \\
&+ \left(M^{-1}T^{-1}\boldsymbol{\omega}'\boldsymbol{J}_T\boldsymbol{\varepsilon}\boldsymbol{\Phi}\right)\boldsymbol{F}_t + \left(M^{-1}T^{-1}\boldsymbol{\omega}'\boldsymbol{J}_T\boldsymbol{\varepsilon}\boldsymbol{\varepsilon}_t\right) \\
&= \boldsymbol{\Lambda}\boldsymbol{\Delta}_F\mathcal{P}\boldsymbol{F}_t + \boldsymbol{O}_p\left(\delta_{MT}^{-1}\right)
\end{aligned}$$

The final line follows directly from Lemma 1.

Item 2:

$$\begin{aligned}
&M^{-1}T^{-2}\boldsymbol{Z}'\boldsymbol{J}_T\varphi(\boldsymbol{X})\varphi(\boldsymbol{X})'\boldsymbol{J}_T\boldsymbol{y} = \boldsymbol{\Lambda}\left(T^{-1}\boldsymbol{F}'\boldsymbol{J}_T\boldsymbol{F}\right)\left(M^{-1}\boldsymbol{\Phi}'\boldsymbol{\Phi}\right)\left(T^{-1}\boldsymbol{F}'\boldsymbol{J}_T\boldsymbol{F}\right)\boldsymbol{\beta} \\
&+ \boldsymbol{\Lambda}\left(T^{-1}\boldsymbol{F}'\boldsymbol{J}_T\boldsymbol{F}\right)\left(M^{-1}\boldsymbol{\Phi}'\boldsymbol{\Phi}\right)\left(T^{-1}\boldsymbol{F}'\boldsymbol{J}_T\boldsymbol{\eta}\right) + \boldsymbol{\Lambda}\left(T^{-1}\boldsymbol{F}'\boldsymbol{J}_T\boldsymbol{F}\right)\left(M^{-1}T^{-1}\boldsymbol{\Phi}'\boldsymbol{\varepsilon}'\boldsymbol{J}_T\boldsymbol{F}\right)\boldsymbol{\beta} \\
&+ \boldsymbol{\Lambda}\left(T^{-1}\boldsymbol{F}'\boldsymbol{J}_T\boldsymbol{F}\right)\left(M^{-1}T^{-1}\boldsymbol{\Phi}'\boldsymbol{\varepsilon}'\boldsymbol{J}_T\boldsymbol{\eta}\right) + \boldsymbol{\Lambda}\left(M^{-1}T^{-1}\boldsymbol{F}'\boldsymbol{J}_T\boldsymbol{\varepsilon}\boldsymbol{\Phi}\right)\left(T^{-1}\boldsymbol{F}'\boldsymbol{J}_T\boldsymbol{F}\right)\boldsymbol{\beta} \\
&+ \boldsymbol{\Lambda}\left(M^{-1}T^{-1}\boldsymbol{F}'\boldsymbol{J}_T\boldsymbol{\varepsilon}\boldsymbol{\Phi}\right)\left(T^{-1}\boldsymbol{F}'\boldsymbol{J}_T\boldsymbol{\eta}\right) + \boldsymbol{\Lambda}\left(M^{-1}T^{-2}\boldsymbol{F}'\boldsymbol{J}_T\boldsymbol{\varepsilon}\boldsymbol{\varepsilon}'\boldsymbol{J}_T\boldsymbol{F}\right)\boldsymbol{\beta} \\
&+ \boldsymbol{\Lambda}\left(M^{-1}T^{-2}\boldsymbol{F}'\boldsymbol{J}_T\boldsymbol{\varepsilon}\boldsymbol{\varepsilon}'\boldsymbol{J}_T\boldsymbol{\eta}\right) + \left(T^{-1}\boldsymbol{\omega}'\boldsymbol{J}_T\boldsymbol{F}\right)\left(M^{-1}\boldsymbol{\Phi}'\boldsymbol{\Phi}\right)\left(T^{-1}\boldsymbol{F}'\boldsymbol{J}_T\boldsymbol{F}\right)\boldsymbol{\beta} \\
&+ \left(T^{-1}\boldsymbol{\omega}'\boldsymbol{J}_T\boldsymbol{F}\right)\left(M^{-1}\boldsymbol{\Phi}'\boldsymbol{\Phi}\right)\left(T^{-1}\boldsymbol{F}'\boldsymbol{J}_T\boldsymbol{\eta}\right) + \left(T^{-1}\boldsymbol{\omega}'\boldsymbol{J}_T\boldsymbol{F}\right)\left(M^{-1}T^{-1}\boldsymbol{\Phi}'\boldsymbol{\varepsilon}'\boldsymbol{J}_T\boldsymbol{F}\right)\boldsymbol{\beta} \\
&+ \left(T^{-1}\boldsymbol{\omega}'\boldsymbol{J}_T\boldsymbol{F}\right)\left(M^{-1}T^{-1}\boldsymbol{\Phi}'\boldsymbol{\varepsilon}'\boldsymbol{J}_T\boldsymbol{\eta}\right) + \left(M^{-1}T^{-1}\boldsymbol{\omega}'\boldsymbol{J}_T\boldsymbol{\varepsilon}\boldsymbol{\Phi}\right)\left(T^{-1}\boldsymbol{F}'\boldsymbol{J}_T\boldsymbol{F}\right)\boldsymbol{\beta} \\
&+ \left(M^{-1}T^{-1}\boldsymbol{\omega}'\boldsymbol{J}_T\boldsymbol{\varepsilon}\boldsymbol{\Phi}\right)\left(T^{-1}\boldsymbol{F}'\boldsymbol{J}_T\boldsymbol{\eta}\right) + \left(M^{-1}T^{-2}\boldsymbol{\omega}'\boldsymbol{J}_T\boldsymbol{\varepsilon}\boldsymbol{\varepsilon}'\boldsymbol{J}_T\boldsymbol{F}\right)\boldsymbol{\beta} \\
&+ \left(M^{-1}T^{-2}\boldsymbol{\omega}'\boldsymbol{J}_T\boldsymbol{\varepsilon}\boldsymbol{\varepsilon}'\boldsymbol{J}_T\boldsymbol{\eta}\right) \\
&= \boldsymbol{\Lambda}\boldsymbol{\Delta}_F\mathcal{P}\boldsymbol{\Delta}_F\boldsymbol{\beta} + \boldsymbol{O}_p\left(\delta_{MT}^{-1}\right)
\end{aligned}$$

The final line follows directly from Lemma 2.

Item 3: Let $= \hat{\boldsymbol{F}}_{C,t} = M^{-1}T^{-1}\boldsymbol{Z}'\boldsymbol{J}_T\varphi(\boldsymbol{X})\varphi(\boldsymbol{x}_t)$. Then, given Lemma 2.1, standard arguments would imply that $M^{-2}T^{-3}\boldsymbol{Z}'\boldsymbol{J}_T\varphi(\boldsymbol{X})\varphi(\boldsymbol{X})'\boldsymbol{J}_T\varphi(\boldsymbol{X})\varphi(\boldsymbol{X})'\boldsymbol{J}_T\boldsymbol{Z} = \dfrac{\hat{\boldsymbol{F}}_C\boldsymbol{J}_T\hat{\boldsymbol{F}}_C'}{T}$

$= \boldsymbol{\Lambda}\boldsymbol{\Delta}_F\mathcal{P}\left(T^{-1}\boldsymbol{F}\boldsymbol{J}_T\boldsymbol{F}\right)\mathcal{P}\boldsymbol{\Delta}_F\boldsymbol{\Lambda}' + \boldsymbol{O}_p\left(\delta_{MT}^{-1}\right)$. Given Assumption 2.1, we have that $\boldsymbol{\Lambda}\boldsymbol{\Delta}_F\mathcal{P}\left(T^{-1}\boldsymbol{F}\boldsymbol{J}_T\boldsymbol{F}\right)\mathcal{P}\boldsymbol{\Delta}_F\boldsymbol{\Lambda}' = \boldsymbol{\Lambda}\boldsymbol{\Delta}_F\mathcal{P}\boldsymbol{\Delta}_F\mathcal{P}\boldsymbol{\Delta}_F\boldsymbol{\Lambda}' + \boldsymbol{O}_p\left(T^{-1/2}\right)$.

Therefore, we have that, $M^{-2}T^{-3}\boldsymbol{Z}'\boldsymbol{J}_T\varphi(\boldsymbol{X})\varphi(\boldsymbol{X})'\boldsymbol{J}_T\varphi(\boldsymbol{X})\varphi(\boldsymbol{X})'\boldsymbol{J}_T\boldsymbol{Z} = \boldsymbol{\Lambda}\boldsymbol{\Delta}_F\mathcal{P}\boldsymbol{\Delta}_F\mathcal{P}\boldsymbol{\Delta}_F\boldsymbol{\Lambda}' + \boldsymbol{O}_p\left(\delta_{MT}^{-1}\right) + \boldsymbol{O}_p\left(T^{-1/2}\right) = \boldsymbol{O}_p\left(\delta_{MT}^{-1}\right)$.

Theorem 1 If Assumption 1-5 hold, we have

$$\hat{\boldsymbol{F}}_t - \boldsymbol{H}_f\boldsymbol{f}_t = \boldsymbol{O}_p(\delta_{MT}^{-1})$$

where $\boldsymbol{H}_f \equiv \hat{\boldsymbol{F}}_A\hat{\boldsymbol{F}}_B^{-1}\boldsymbol{\Lambda}\boldsymbol{\Delta}_F\mathcal{P}$

$\hat{\boldsymbol{F}}_A = T^{-1}\boldsymbol{Z}'\boldsymbol{J}_T\boldsymbol{Z}$ and

$\hat{\boldsymbol{F}}_B = M^{-1}T^{-2}\boldsymbol{Z}'\boldsymbol{J}_T\varphi(\boldsymbol{X})\varphi(\boldsymbol{X}')\boldsymbol{J}_T\boldsymbol{Z}$

Proof:

$$\begin{aligned}
\hat{\boldsymbol{F}}_t &= T^{-1}\boldsymbol{Z}'\boldsymbol{J}_T\boldsymbol{Z}\left(M^{-1}T^{-2}\boldsymbol{Z}'\boldsymbol{J}_T\varphi(\boldsymbol{X})\varphi(\boldsymbol{X})'\boldsymbol{J}_T\boldsymbol{Z}\right)^{-1}M^{-1}T^{-1}\boldsymbol{Z}'\boldsymbol{J}_T\varphi(\boldsymbol{X})\varphi(\boldsymbol{x}_t) \\
&= \hat{\boldsymbol{F}}_A\hat{\boldsymbol{F}}_B^{-1}\left(\boldsymbol{\Lambda}\boldsymbol{\Delta}_F\mathcal{P}\boldsymbol{F}_t + \boldsymbol{O}_p\left(\delta_{MT}^{-1}\right)\right) \\
&= \hat{\boldsymbol{F}}_A\hat{\boldsymbol{F}}_B^{-1}\boldsymbol{\Lambda}\boldsymbol{\Delta}_F\mathcal{P}\boldsymbol{F}_t + \boldsymbol{O}_p\left(\delta_{MT}^{-1}\right) \\
&= \boldsymbol{H}_f\boldsymbol{f}_t + \boldsymbol{O}_p(\delta_{MT}^{-1})
\end{aligned}$$

The second equality follows from Lemma 2.1 and the final equality uses the definition of $\boldsymbol{H}_f$.

Theorem 2 If Assumption 1-5 hold, we have

$$\hat{\boldsymbol{\beta}} - \boldsymbol{G}_\beta\boldsymbol{\beta} = \boldsymbol{O}_p(\delta_{MT}^{-1}).$$

where $\boldsymbol{G}_\beta \equiv \hat{\boldsymbol{\beta}}_1^{-1}\hat{\boldsymbol{\beta}}_2\left[\boldsymbol{\Lambda}\boldsymbol{\Delta}_F\mathcal{P}\boldsymbol{\Delta}_F\mathcal{P}\boldsymbol{\Delta}_F\boldsymbol{\Lambda}'\right]^{-1}\boldsymbol{\Lambda}\boldsymbol{\Delta}_F\mathcal{P}\boldsymbol{\Delta}_F$,

$\hat{\boldsymbol{\beta}}_1 = \hat{\boldsymbol{F}}_A$ and $\hat{\boldsymbol{\beta}}_2 = \hat{\boldsymbol{F}}_B$

Proof:

$$
\begin{aligned}
\hat{\boldsymbol{\beta}} &= \left(T^{-1}\boldsymbol{Z}'\boldsymbol{J}_T\boldsymbol{Z}\right)^{-1} M^{-1}T^{-2}\boldsymbol{Z}'\boldsymbol{J}_T\varphi(\boldsymbol{X})\varphi(\boldsymbol{X})'\boldsymbol{J}_T\boldsymbol{Z} \\
&\times \left(M^{-2}T^{-3}\boldsymbol{Z}'\boldsymbol{J}_T\varphi(\boldsymbol{X})\varphi(\boldsymbol{X})'\boldsymbol{J}_T\varphi(\boldsymbol{X})\varphi(\boldsymbol{X})'\boldsymbol{J}_T\boldsymbol{Z}\right)^{-1} M^{-1}T^{-2}\boldsymbol{Z}'\boldsymbol{J}_T\varphi(\boldsymbol{X})\varphi(\boldsymbol{X})'\boldsymbol{J}_T\boldsymbol{y} \\
&= \hat{\boldsymbol{\beta}}_1^{-1}\hat{\boldsymbol{\beta}}_2\left(\boldsymbol{\Lambda}\boldsymbol{\Delta}_F\mathcal{P}\boldsymbol{\Delta}_F\mathcal{P}\boldsymbol{\Delta}_F\boldsymbol{\Lambda}' + \boldsymbol{O}_p\left(\delta_{MT}^{-1}\right)\right)^{-1}\left(\boldsymbol{\Lambda}\boldsymbol{\Delta}_F\mathcal{P}\boldsymbol{\Delta}_F\boldsymbol{\beta} + \boldsymbol{O}_p\left(\delta_{MT}^{-1}\right)\right) \\
&= \hat{\boldsymbol{\beta}}_1^{-1}\hat{\boldsymbol{\beta}}_2\left[\left(\boldsymbol{\Lambda}\boldsymbol{\Delta}_F\mathcal{P}\boldsymbol{\Delta}_F\mathcal{P}\boldsymbol{\Delta}_F\boldsymbol{\Lambda}'\right)^{-1} - \left(\boldsymbol{\Lambda}\boldsymbol{\Delta}_F\mathcal{P}\boldsymbol{\Delta}_F\mathcal{P}\boldsymbol{\Delta}_F\boldsymbol{\Lambda}'\right)^{-1}\boldsymbol{O}_p\left(\delta_{MT}^{-1}\right)\left(\boldsymbol{O}_p(1) + \boldsymbol{O}_p\left(\delta_{MT}^{-1}\right)\right)^{-1}\right] \times \\
&\left(\boldsymbol{\Lambda}\boldsymbol{\Delta}_F\mathcal{P}\boldsymbol{\Delta}_F\boldsymbol{\beta} + \boldsymbol{O}_p\left(\delta_{MT}^{-1}\right)\right) \\
&= \hat{\boldsymbol{\beta}}_1^{-1}\hat{\boldsymbol{\beta}}_2\left[\boldsymbol{\Lambda}\boldsymbol{\Delta}_F\mathcal{P}\boldsymbol{\Delta}_F\mathcal{P}\boldsymbol{\Delta}_F\boldsymbol{\Lambda}'\right]^{-1}\boldsymbol{\Lambda}\boldsymbol{\Delta}_F\mathcal{P}\boldsymbol{\Delta}_F\boldsymbol{\beta} + \boldsymbol{O}_p\left(\delta_{MT}^{-1}\right) \\
&= \boldsymbol{G}_\beta\boldsymbol{\beta} + \boldsymbol{O}_p(\delta_{MT}^{-1})
\end{aligned}
$$

where the second equality employs Lemma 2.2 and 2.3. The third equality uses the fact that for any invertible matrices $\boldsymbol{A}$ and $\boldsymbol{A}+\boldsymbol{B}$ we have $(\boldsymbol{A}+\boldsymbol{B})^{-1} = \boldsymbol{A}^{-1} - \boldsymbol{A}^{-1}\boldsymbol{B}(\boldsymbol{A}+\boldsymbol{B})^{-1}$, which in our case implies that,
$\left(\boldsymbol{\Lambda}\boldsymbol{\Delta}_F\mathcal{P}\boldsymbol{\Delta}_F\mathcal{P}\boldsymbol{\Delta}_F\boldsymbol{\Lambda}' + \boldsymbol{O}_p(\delta_{MT}^{-1})\right)^{-1} =$
$(\boldsymbol{\Lambda}\boldsymbol{\Delta}_F\mathcal{P}\boldsymbol{\Delta}_F\mathcal{P}\boldsymbol{\Delta}_F\boldsymbol{\Lambda}')^{-1} - (\boldsymbol{\Lambda}\boldsymbol{\Delta}_F\mathcal{P}\boldsymbol{\Delta}_F\mathcal{P}\boldsymbol{\Delta}_F\boldsymbol{\Lambda}')^{-1}\boldsymbol{O}_p(\delta_{MT}^{-1})\left(\boldsymbol{\Lambda}\boldsymbol{\Delta}_F\mathcal{P}\boldsymbol{\Delta}_F\mathcal{P}\boldsymbol{\Delta}_F\boldsymbol{\Lambda}' + \boldsymbol{O}_p(\delta_{MT}^{-1})\right)^{-1}.$
The last equality uses the definition of $\boldsymbol{G}_\beta$.

Theorem 3 If Assumption 1-5 hold, we have

$$\hat{y}_{t+h} - \mathbb{E}_t y_{t+h} = O_p(\delta_{MT}^{-1})$$

Proof:

$$
\begin{aligned}
\hat{y}_{t+h} &= \bar{y} + \boldsymbol{J}_T \hat{\boldsymbol{F}}_T' \hat{\boldsymbol{\beta}} \\
&= \beta_0 + \bar{\boldsymbol{f}}' \boldsymbol{\beta}_f + O_p(T^{-1/2}) + \left(\boldsymbol{H}_f \boldsymbol{f}_t + \boldsymbol{O}_p(\Gamma_{NT}^{-1})\right)' \left(\boldsymbol{G}_\beta \boldsymbol{\beta} + \boldsymbol{O}_p(\delta_{MT}^{-1})\right) \\
&= \beta_0 + \bar{\boldsymbol{f}}' \boldsymbol{\beta}_f + \left(\boldsymbol{f}_t - \bar{\boldsymbol{f}}\right)' \boldsymbol{H}_f' \boldsymbol{G}_\beta \boldsymbol{\beta} + \boldsymbol{O}_p(\delta_{MT}^{-1}) \\
&= \beta_0 + \bar{\boldsymbol{f}}' \boldsymbol{\beta}_f + \left(\boldsymbol{f}_t - \bar{\boldsymbol{f}}\right)' \boldsymbol{\beta} + \boldsymbol{O}_p(\delta_{MT}^{-1}) \\
&= \beta_0 + \boldsymbol{f}_t' \boldsymbol{\beta} + \boldsymbol{O}_p(\delta_{MT}^{-1}) \\
&= \mathbb{E}_t y_{t+h} + O_p(\delta_{MT}^{-1})
\end{aligned}
$$

The second equality follows from lemma 1.15. The fourth equality follows if $\boldsymbol{H}_f' \boldsymbol{G}_\beta$ is an identity matrix. This is indeed true since $\boldsymbol{H}_f' \boldsymbol{G}_\beta = \mathcal{P} \boldsymbol{\Delta}_F \boldsymbol{\Lambda}' \left[\boldsymbol{\Lambda} \boldsymbol{\Delta}_F \mathcal{P} \boldsymbol{\Delta}_F \mathcal{P} \boldsymbol{\Delta}_F \boldsymbol{\Lambda}'\right]^{-1} \boldsymbol{\Lambda} \boldsymbol{\Delta}_F \mathcal{P} \boldsymbol{\Delta}_F$. Using the arguments as in Lemma 5 and Theorem 1 of Kelly & Pruitt (2015) the RHS is an identity matrix, given assumptions 4 and 5.

A.2 Mercer's Theorem

Suppose $\mathcal{X} \subseteq \mathbb{R}^d$ is compact and kernel function $\mathcal{K} : \mathcal{X} \times \mathcal{X} \to \mathbb{R}$ is continuous, satisfying the following conditions,

$$
\int_{\mathrm{y}} \int_{\mathrm{x}} \mathcal{K}^2(\mathrm{x}, \mathrm{y}) d\mathrm{x} d\mathrm{y} < \infty \quad \text{ and } \quad \int_{\mathrm{y}} \int_{\mathrm{x}} h(\mathrm{x}) \mathcal{K}(\mathrm{x}, \mathrm{y}) h(\mathrm{y}) d\mathrm{x} d\mathrm{y} \geq 0, \quad \forall h \in L^2(\mathcal{X}),
$$

where $L^2(\mathcal{X}) = \left\{h : \int h^2(\mathrm{s}) ds < \infty\right\}$, then there exist functions $\left\{\varphi_i(\cdot) \in L^2(\mathcal{X}), i = 1, 2, \ldots\right\}$ and non-negative coefficients $\theta_1 \geq \theta_2 \geq \ldots \geq 0$ which together forms an orthonormal system in $L^2(\mathcal{X})$, i.e. $\langle \varphi_i, \varphi_j \rangle_{L^2(\mathcal{X})} = \int \varphi_i(\mathrm{x}) \varphi_j(\mathrm{x}) d\mathrm{x} = \mathbb{I}_{\{i=j\}}$, such that

$$
\mathcal{K}(\mathrm{x}, \mathrm{y}) = \sum_{i=1}^{\infty} \theta_i \varphi_i(\mathrm{x}) \varphi_i(\mathrm{y}), \quad \forall \mathrm{x}, \mathrm{y} \in \mathcal{X}
$$

B Algorithms, Data, and Figures

This appendix provides algorithmic details, data sources, transformation, and visual plots.

B.1 Out of Sample Estimation

We train our model on in-sample information and then construct a sample forecast, as discussed in the algorithm below.

Step	Description
1	Take in-sample data $\{\boldsymbol{X}_{in}, \boldsymbol{y}_{in}\}$ out-of-sample predictor matrix $\boldsymbol{X}_{out}$ and proxy matrix $\boldsymbol{Z}$.
2	Compute the following two kernel matrices: $\mathbf{K}_{in} = \mathcal{K}(\boldsymbol{X}_{in}, \boldsymbol{X}_{in})$ and $\mathbf{K}_{out} = \mathcal{K}(\boldsymbol{X}_{in}, \boldsymbol{X}_{out})$
3	Estimate in and out of the sample factor matrix using the following formula: $\widehat{\boldsymbol{F}}_{in} = \big(\boldsymbol{Z}'\boldsymbol{J}_T\boldsymbol{Z}\big)\big(\boldsymbol{Z}'\boldsymbol{J}_T\mathbf{K}_{in}\boldsymbol{J}_T\boldsymbol{Z}\big)^{-1}\big(\boldsymbol{Z}'\boldsymbol{J}_T\mathbf{K}_{in}\big)$ $\widehat{\boldsymbol{F}}_{out} = \big(\boldsymbol{Z}'\boldsymbol{J}_T\boldsymbol{Z}\big)\big(\boldsymbol{Z}'\boldsymbol{J}_T\mathbf{K}_{in}\boldsymbol{J}_T\boldsymbol{Z}\big)^{-1}\big(\boldsymbol{Z}'\boldsymbol{J}_T\mathbf{K}_{out}\big)$ To accommodate the intercept term in pass-3, Compute a modified factor matrix estimate $\widetilde{\boldsymbol{F}}_{in} = [\mathbf{1} \quad \widehat{\boldsymbol{F}}_{in}]$ and $\widetilde{\boldsymbol{F}}_{out} = [\mathbf{1} \quad \widehat{\boldsymbol{F}}_{out}]$, where $\mathbf{1}$ is a vector of ones.
4	Estimate $\boldsymbol{\beta}$ using the following formula: $\widehat{\boldsymbol{\beta}} = \Big(\widetilde{\boldsymbol{F}}'_{in}\widetilde{\boldsymbol{F}}_{in}\Big)^{-1}\widetilde{\boldsymbol{F}}_{in}\boldsymbol{y}_{in}$ (this $\widehat{\boldsymbol{\beta}}$ contains intercept term as well and is estimated in-sample).
5	Obtain out-of-sample forecast: $\widehat{\boldsymbol{y}}_{t+h} = \widetilde{\boldsymbol{F}}_{out}\widehat{\boldsymbol{\beta}}$

Table 13: Algorithm: The Out-of-sample forecast by Kernel Three Pass Regression Filter

We have demonstrated the construction of an out-of-sample forecast (Table-13). Now, we outline the rolling window procedure to obtain the out-of-sample forecast performance measured by out-of-sample R^2 in Table-14.

B.2 Data Source and Description

We use FRED-QD data. This section provides the codes of the variables we forecast in our empirical work. For detailed description details, refer to FRED website. In table-15, FRED means federal reserve economic data, and SW stands for Stock and Watson datasets.

Step	Description
1	**Get Input Data and Parameters**
	We forecast h period(s) ahead w is the number of training observations.
	Get $T \times N$ matrix $\mathbf{X}$: matrix of predictors, and $T \times 1$ vector $\mathbf{y}$: target series.
2	**Run Rolling Windows**
	Loop Begins: j from 1 to $test\_size$
	i) Set training and test using as follows:
	$\mathbf{y}_{train} = \mathbf{y}[(j+h) : (j+w+h-1)]$
	$\mathbf{X}_{train} = \mathbf{X}[j : (w+j-1)]$ and $\mathbf{X}_{test} = \mathbf{X}[(w+j)]$
	ii) Train the model on $\{\mathbf{X}_{train}, \mathbf{y}_{train}\}$. Obtain $\tilde{F}_{oos}$ and $\hat{\beta}_{in}$
	iii) Obtain the forecast $\widehat{y} = \tilde{F}'_{oos}\hat{\beta}_{in}$
	iv) Obtain $\mathbf{y}_{pred}[j] = \widehat{y}$, $\mathbf{y}_{oos}[j] = \mathbf{y}[j+w+h]$, and $\mathbf{y}_{mean}[j] = mean(\mathbf{y}_{train})$
	Loop Ends
3	**Compute Out-of-sample** R^2:
	i) Calculate the sum of squared residuals of the model
	$SSR_{model} = \sum_{j=1}^{test\_size} \Big(\mathbf{y}_{oos}[j] - \mathbf{y}_{pred}[j]\Big)^2$
	ii) Get sum of squared residuals of historical mean
	$SSR_{hist} = \sum_{j=1}^{test\_size} \Big(\mathbf{y}_{oos}[j] - \mathbf{y}_{mean}[j]\Big)^2$
	iii) Obtain out of sample R^2: $R^2 = 1 - \frac{SSR_{model}}{SSR_{hist}}$

Table 14: Rolling Window Procedure to Calculate Out of Sample R^2

	FRED Mnemonic	SW Mnemonic	Description
Macro			
	GDPC1	GDP	Real Gross Domestic Product, 3 Decimal (Billions of Chained 2012 Dollars)
	PCECC96	Consumption	Real Personal Consumption Expenditures (Billions of Chained 2012 Dollars)
	EXPGSC1	Exports	Real Exports of Goods & Services, 3 Decimal (Billions of Chained 2012 Dollars)
	IMPGSC1	Imports	Real Imports of Goods & Services, 3 Decimal (Billions of Chained 2012 Dollars)
	GPDIC1	Investment	Real Gross Private Domestic Investment, 3 decimal (Billions of Chained 2012 Dollars)
	FPIx	FixedInv	Real private fixed investment (Billions of Chained 2012 Dollars), deflated using PCE
	IPFINAL	IP:Final products	Industrial Production: Final Products (Market Group) (Index 2012=100)
Labor			
	PAYEMS	Emp:Nonfarm	All Employees: Total nonfarm (Thousands of Persons)
	UNRATE	Unemp Rate	Civilian Unemployment Rate (Percent)
Housing			
	HOUST	Hstarts	Housing Starts: Total: New Privately Owned Housing Units Started (Thousands of Units)
	HOUSTW	Hstarts:W	Housing Starts in West Census Region (Thousands of Units)
Price			
	GDPCTPI	GDP Defl	Gross Domestic Product: Chain-type Price Index (Index 2012=100)
	CPIAUCSL	CPI	Consumer Price Index for All Urban Consumers: All Items (Index 1982-84=100)
Finance			
	GS1	TB-1YR	1-Year Treasury Constant Maturity Rate(%)
	GS10	TB-10YR	10-Year Treasury Constant Maturity Rate (%)
	S&P 500		S&P's Common Stock Price Index: Composite

Table 15: Variable Mnemonic and Description

B.3 Hyper-parameter Tuning Algorithm

The following table demonstrates our algorithm to tune hyper-parameters σ.

Take an appropriate range of σ say $\sigma \in \{0.001, 0.002, 0.003, ..., 14.998, 14.999, 15\}$.

For each value of σ_j do the following:

0. Initialize two variables $R^2_{best} = 0$ and $\sigma_{best} = 0.001$

1. Take training input data $\{X_{train}, y_{train}\}$ and split it into two halves:

   $\{X_{train1}, y_{train1}\}$ and $\{X_{train2}, y_{train2}\}$.

   One half works as a training set, and the other as a validation set.

2. i) For given σ_j, train the model on $\{X_{train1}, y_{train1}\}$ and

   obtain forecast $\hat{y}_{t+h}$ on $\{X_{train2}, y_{train2}\}$.

   ii) Obtain R^2 from comparison of $\hat{y}_{t+h}$ and y_{t+h} and call it R^2_1.

   iii) Repeat the procedure by flipping training and validation sets and obtain R^2_2.

   iv) Obtain $R^2_{\sigma_j} = \frac{R^2_1 + R^2_2}{2}$. If $R^2_{\sigma_j} > R^2_{best}$, update $\sigma_{best} = \sigma_j$ and $R^2_{best} = R^2_{\sigma_j}$.

3. Repeat the step-1 and step-2 for all value of σ_j and return the σ_{best}.

Table 16: Cross-Validation Based Hyper-Parameter Tuning Algorithm

We employ a two-fold cross-validation approach to optimize the hyperparameters. While widely used, traditional K-fold cross-validation is suboptimal for time series data due to its inherent sequential structure. Instead, for our primary analysis, we adopt a rolling window methodology. However, we resort to a fixed-window two-fold cross-validation strategy to mitigate computational expenses. Notably, we compared the computational costs and performance gains of the rolling-window tuning algorithm and the two-fold cross-validation approach.

B.4 Comparative Forecast Performance

We plot the forecasts by our method and 3PRF method with the true value of the target series for all sixteen series discussed in the emprirical application section. To save some space, we only show the plots for one, four, eight, and twelve period ahead forecasts.

Figure 5: One Period Ahead Forecasting: Comparative Performance

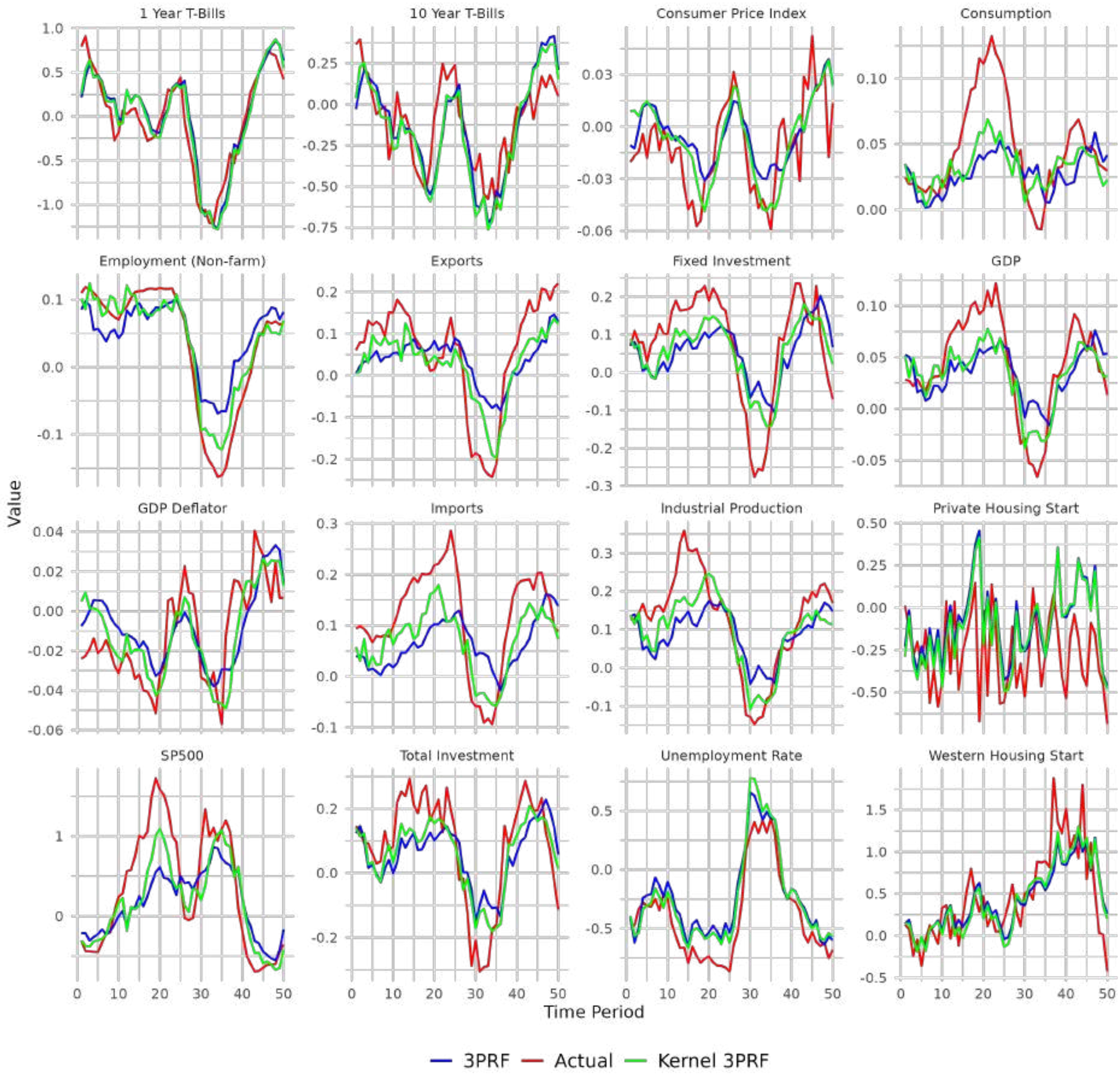

Figure 6: Four Period Ahead Forecasting: Comparative Performance

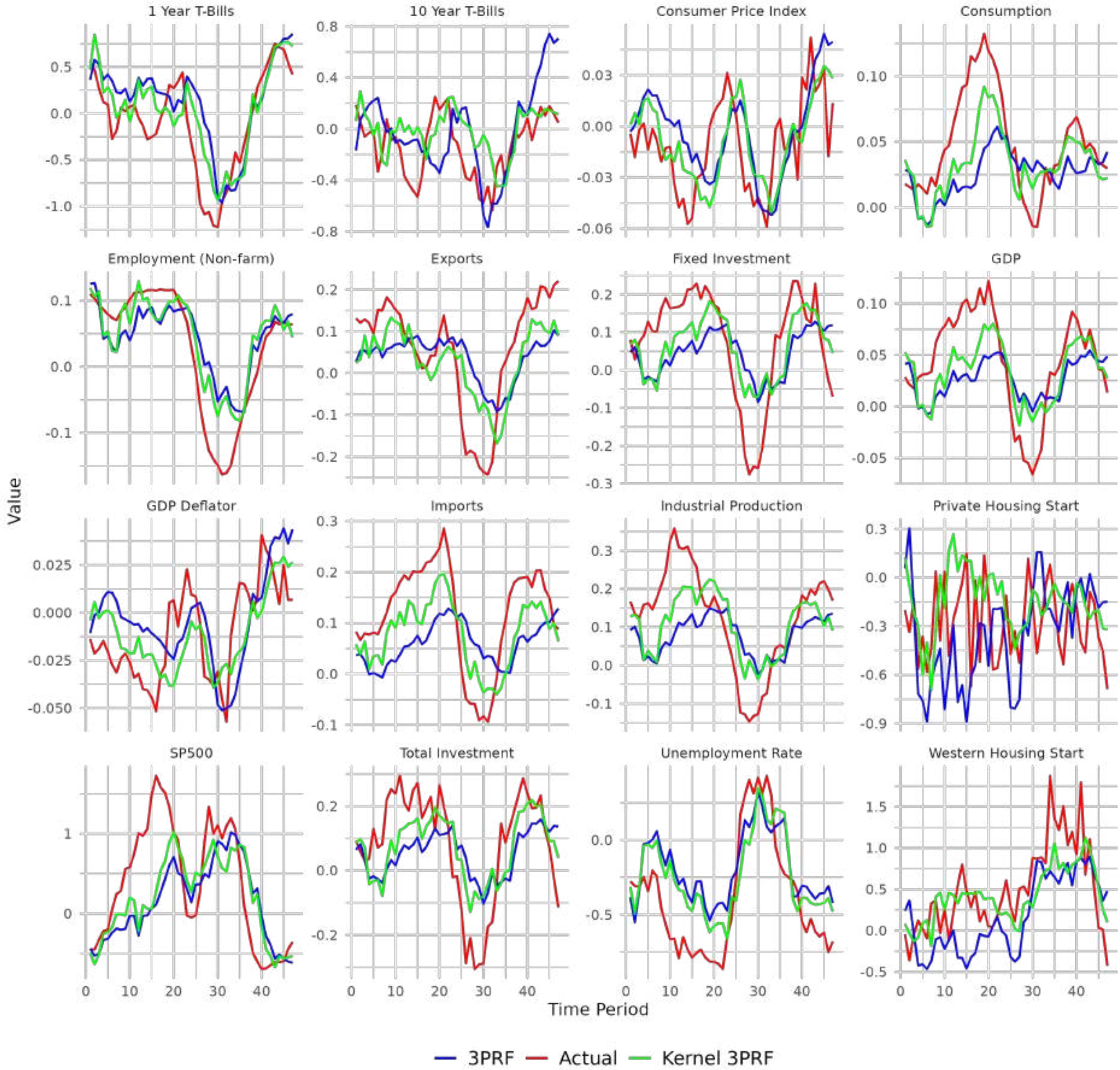

B.5 Comparative Performance on All Series For Each Horizons

Figure 7: Eight Period Ahead Forecasting: Comparative Performance

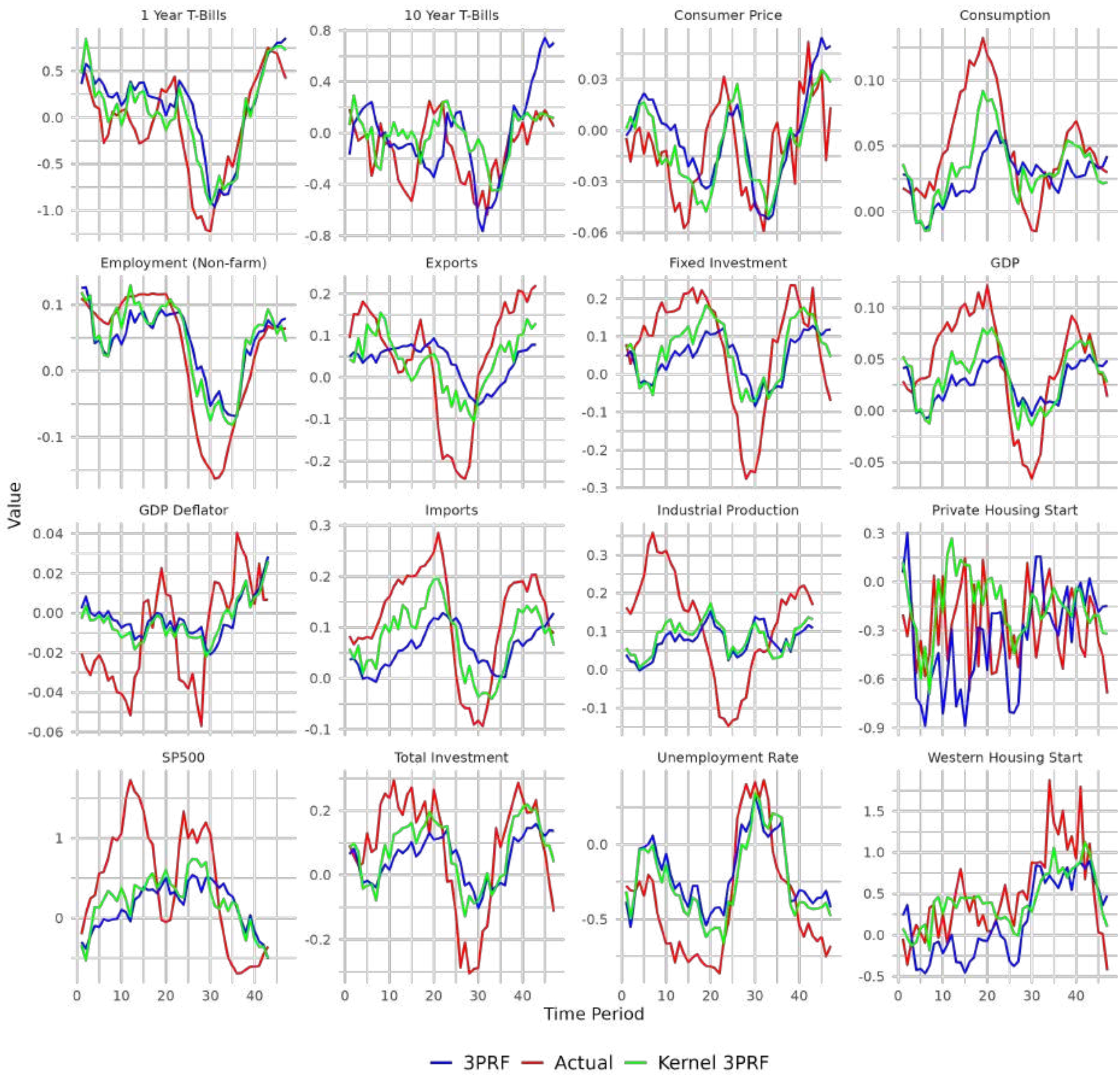

Figure 8: Twelve Period Ahead Forecasting: Comparative Performance

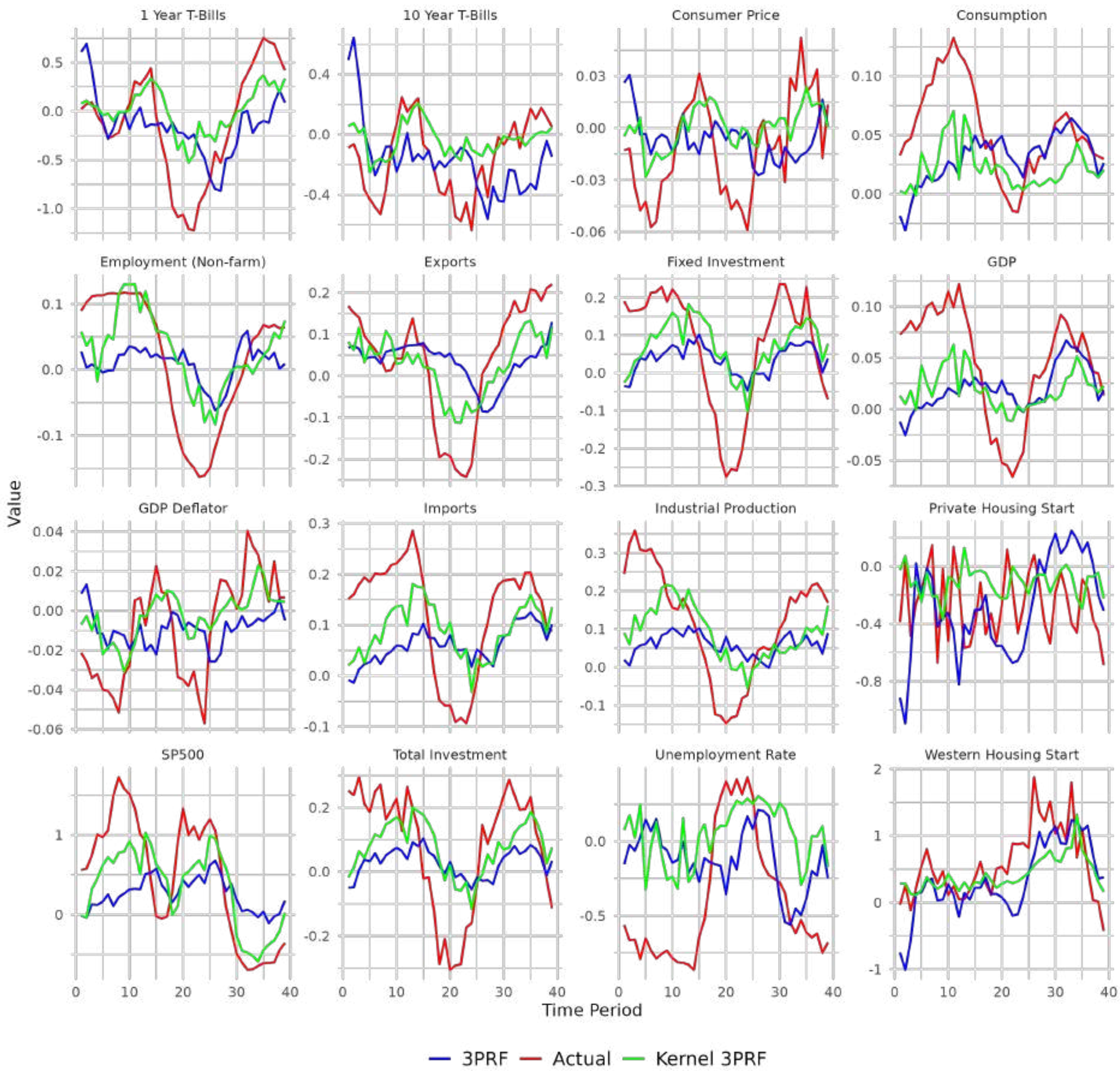

Analysis	Tolerance(%)	Methods						
		AR(2)	**PCA**	**Sq-PC**	**PC-Sq**	**kPCA**	**3PRF**	**k3PRF**
h=1								
	0	93.75	0.00	0.57	0.00	0.00	0.57	5.11
	5	95.45	1.70	0.00	0.57	0.57	5.11	11.93
	10	97.73	4.55	0.57	3.41	2.27	13.07	23.86
	20	97.73	13.07	3.41	14.20	4.55	23.86	49.43
h=2								
	0	93.75	0.00	0.00	0.57	0.57	1.70	3.41
	5	95.45	1.14	0.00	1.70	0.57	4.55	8.52
	10	95.45	2.84	1.70	3.98	1.70	6.82	13.64
	20	96.59	9.09	2.84	10.80	4.55	16.48	40.91
h=3								
	0	84.09	0.57	0.57	0.57	0.00	2.27	11.93
	5	89.20	1.70	1.14	2.27	0.00	3.98	19.89
	10	93.18	2.84	2.27	4.55	0.00	7.39	27.27
	20	94.89	6.25	3.41	9.66	1.70	17.61	47.16
h=4								
	0	64.77	0.00	0.57	1.14	1.14	2.27	30.11
	5	68.18	1.14	1.70	1.70	1.14	6.82	34.66
	10	76.70	2.84	2.27	3.41	1.14	9.66	39.77
	20	88.07	5.11	3.98	6.82	3.41	22.16	57.39
h=6								
	0	27.84	0.00	2.84	0.00	8.52	6.25	53.98
	5	29.55	0.00	3.98	1.70	9.66	7.95	58.52
	10	32.39	1.14	5.11	2.84	10.80	14.77	61.36
	20	40.91	5.11	6.82	7.39	14.20	25.00	70.45
h=8								
	0	9.09	0.57	1.14	2.27	7.39	9.66	69.89
	5	9.66	2.27	1.70	2.84	8.52	11.36	70.45
	10	10.23	2.84	1.70	2.84	11.36	15.34	72.16
	20	11.36	3.41	4.55	5.11	13.07	28.41	78.98
h=10								
	0	8.52	0.00	0.57	2.84	3.98	18.18	65.91
	5	8.52	0.00	1.14	2.27	3.98	19.89	67.61
	10	9.09	0.00	1.70	2.27	3.98	22.73	68.75
	20	9.66	1.14	2.27	3.98	7.95	29.55	73.30
h=12								
	0	3.98	0.57	0.57	3.41	2.27	13.07	76.14
	5	4.55	1.14	1.14	2.84	2.27	13.64	76.70
	10	4.55	1.14	1.70	3.41	2.84	14.77	80.11
	20	6.25	2.27	2.27	3.98	4.55	23.30	82.95

Table 17: Distribution of Best Forecasting Methods Across All Series in Our Data (Percentage)